CHAPTER 2

Theory and literature review

In this chapter, the background and the theoretical framework of ferroelectric glass-ceramics are proposed. The ferroelectric material from potassium sodium niobate has been subjected to intensive studied due to its interesting properties such as the electrical and optical properties. The chapter starts with the background of ferroelectric property which is necessary for understanding the overviews of this research. Then, the glass and glass-ceramic kinetics are carried out based on the literature reviews. Therefore, in order to improve the electrical and the optical properties of glass-ceramics, the incorporation method was brought into glass preparation process. Moreover, the effects of rare-earth dopant in glass and glass-ceramics to the properties are also reviewed and concluded in this chapter.

2.1 Ferroelectric property for glass-ceramics

Ferroelectric crystals are useful materials in opto-electronic devices because of the integration between the remarkable optical and electrical properties. The special of their structure (non-centrosymmetric) bring to the presence of many nonlinear optical properties, such as, the electro-optic effect (change in refractive index with electric field), harmonic generation (change in frequency of light), and photorefraction (change of refractive index response to light) and etc.

ลิขสิทธิ์มหาวิทยาลัยเชียงใหม่
Copyright© by Chiang Mai University
All rights reserved

Recently, much attention has been paid on the development of transparent ferroelectric glass-ceramics (TFGCs) to replaced transparent single crystal. The reason is the high cost of production process and the difficulty to prepare single crystal. With the glass preparation technology, the high speed production line can be achieved, giving the low-cost fabrication and good performance transparent materials. The aimed of mixed ferroelectric crystal with glass is to generate the glass-ceramics which combine the electrical and optical properties of ferroelectric crystals and transparency of glass

together. Next topics are the explanation of ferroelectric property following by the glass-ceramics kinetics.

2.1.1 Ferroelectric characteristic

Ferroelectrics (FE) are materials in which showed their own electric spontaneous polarization (P_s). This spontaneous polarization can switch by external electric filed and external mechanical stress. The beginning of the discovery ferroelectricity started with the finding of Rochelle salt (sodium potassium tartrate tetrahydrate) in 1675 by Elie Seignette, France [18,20]. Then, after 400 years of first found Rochelle salt, in 1920, J. Valasek [19] was investigating the dielectric properties of Rochelle salt ($NaKC_4H_4O_6.4H_2O$). He found some electric property in Rochelle salt and called ferroelectricity.

In 1946, A von Hippel et al. [21] and Gray et al. [22] reported that barium titanate ($BaTiO_3$ or BT) also showed ferroelectric property with high dielectric constant. Gray explained the ferroelectric nature of ceramic $BaTiO_3$ that the electric field (E) could change the domain of BT within the grains, making the polycrystalline materials that similar to the single crystal property. This process is called poling. Since then, over 250 materials were found to exhibit ferroelectric properties. The most famous materials include; lead titanate (PT), lead lanthanum zirconate titanate (PLZT), lead zirconate titanate (PZT), lead manganese niobate (PMN) and potassium sodium niobate (KNN) [18,20]. Ferroelectric materials are very useful in many applications especially electronic devices. To be clearly understand about their property, the structures of these material groups need to be studied.

ลิขสิทธิ์มหาวิทยาลัยเชียงใหม่
Copyright© by Chiang Mai University
All rights reserved

Naturally, materials have their own pattern of crystal structure. The crystal structure of ferroelectric material often shows lacking a centre of symmetry or non-centrosymmetric. The centre of symmetry refers to the atoms in the structure arranged to be a unit cell. The non-centrosymmetric point groups are shown in Table 2.1 [23]. All crystalline materials in which their structures possess these point groups, exhibit the phenomenon of piezoelectricity. This is explained that applied stress can generate a charge in the crystal structure

and the release of the stain (mechanical strain) will be shown up after applying electric filed. We have known as the conversion of piezoelectric effect. This phenomenon is widely used in many electronic devices.

Table 2.1 The type of non-polar (non-centrosymmetric) point groups [23].

Crystal system	Polar (acentric)	Nonpolar (acentric)
Triclinic	1	
Monoclinic	2, m	
Orthorhombic	mm2	222
Trigonal	3, 3m	32
Hexagonal	6, 6mm	$\bar{6}$, $\bar{6}$m2
Tetragonal	4, 4mm	$\bar{4}$, 422, $\bar{4}$2m
Cubic	None	23, $\bar{4}$3m , 432

Fig. 2.1 shows that there are 20 non-centrosymmetric crystal groups which exhibits polarizaon under applied stress. This group can be separated into 10 classes of crystal group from the possible 20. These 10 crystal classes called pyroelectric. Pyroelectric group is unique characteristic of material that permanently polarized with the temperature change. The examples of pyroelectric material that we know well are tourmaline and wurtzite. This pyroelectric group can be divided into small subgroups named ferroelectric. The ferroelectric possesses spontaneous dipole moment that converted by E of some magnitude that smaller than dielectric breakdown of the material. Thus, this group is unlike pyroelectric at all. The important factors that we use to classify ferroelectric materials are as follows;

(1) The spontaneous polarization in materials,

(2) The ability of polarization in reorientation.

Ferroelectric ceramics can be divided into 4 types, including the tungsten–bronze group, the oxygen octahedral group, the pyrochlore group, and the bismuth layer–structure group based on their unit-cell structure. The most

ลิขสิทธิ์มหาวิทยาลัยเชียงใหม่
Copyright© by Chiang Mai University
All rights reserved

famous structure of all is the perovskite structure or ABO_3 which is widely used in the manufacturing (i.e. BT, PZT, PLZT, PT, PMN and KNN). A typical ABO_3 structure is given in Fig. 2.3. The characteristics of ferroelectric property can be observed by the hysteresis loops as shown in Fig. 2.2.

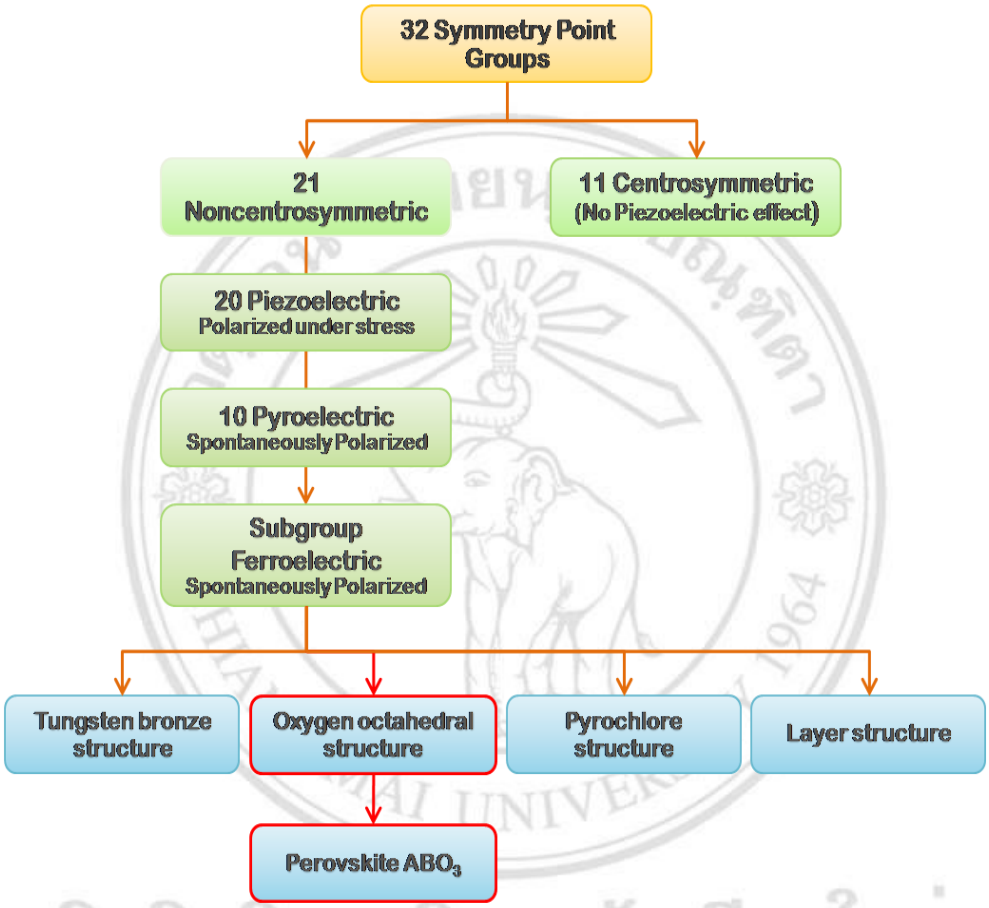

Figure 2.1 The flow-chart of piezoelectric and subgroups divided by structural symmetry [20].

ลิขสิทธิ์มหาวิทยาลัยเชียงใหม่
Copyright© by Chiang Mai University
All rights reserved

The important characteristics of ferroelectric are exhibited via hysteresis loops diagram as shown in Fig. 2.2. The hysteresis loop is the schematic plot between polarization and electric field. From Fig. 2.2, the dipole moment of crystal is aligned into one direction after applied electric field from 0. The alignment is arising until it reaches the saturation point. The increase of polarization (P) is due to the dielectric constant (ε_r) in material. (The gradient of the P/E curve for a linear dielectric is similar to that of its permittivity.)

Extrapolation of this line back to the abscissa gives the saturation value called the spontaneous polarisation (P_s). The decreased of the field to 0 gives the value of the remanent polarisation (P_r), which is normally less than P_s. A negative field decreases the polarization, until it get to 0 at the coercive field ($-E_c$). An additional negative increase of the field causes a reverse saturation polarisation ($-P_s$). When the E returns to 0 the crystal is left with a negative remanent polarisation ($-P_r$). After apply of the E once again, the polarisation then increases from $-P_r$ to 0 at E_c, and then to $+P_s$, completing the ferroelectric hysteresis loop.

Because of the capability of polarization in switching direction, this material is useful in the area of nonvolatile memory application. Moreover, it allows the polycrystalline ferroelectrics to be polarized. The angle of polarization in adjacent area can reached to 180° to each other. Normally, the polarization can be selected between many probable directions so that adjacent regions can have polarizations. The simple directions of polarization under electric field are also shown in Fig. 2.2. The lists of ferroelectrics properties and usages are showed as follows [23]:

1) The hysteresis loop of ferroelectric is used in non-volatile memory for computer information storage.
2) Ferroelectrics can present high relative permittivities (several thousand) which are widely used in capacitors.
3) The direct piezoelectric effect (the applied of stress to generate charge) is used in sensors such as hydrophones, micro-phones, accelerometers etc.
4) The reverse piezoelectric effect (the applied of electric filed responding in generation of strain) is broadly used in filters, ultrasonic generators, resonators, actuators etc.
5) The pyroelectric effect (the change in temperature to generate charge) is broadly used in uncooled infrared detectors.

ลิขสิทธิ์มหาวิทยาลัยเชียงใหม่
Copyright© by Chiang Mai University
All rights reserved

6) The electro-optic effect (the applied electric filed can change birefringence properties) is useful for optical shutters, integrated optical (photonic) devices and laser Q-switches.

7) The non-linear optical effects from ferroelectrics are useful for optical mixing and laser frequency doubling.

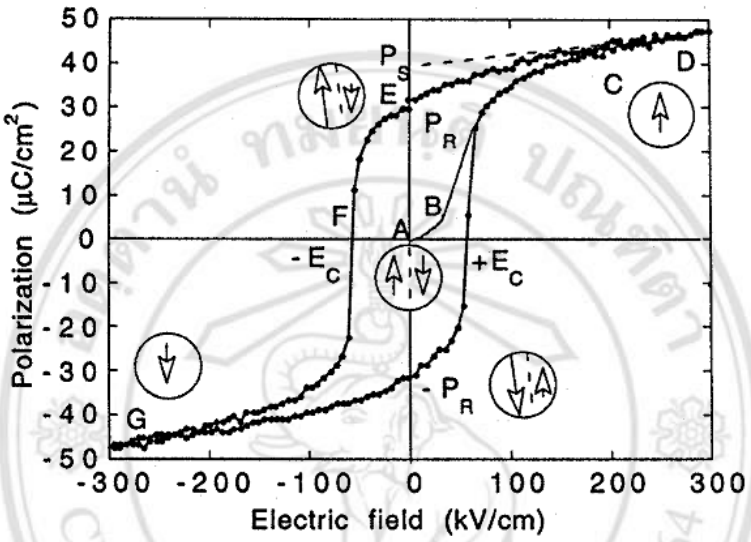

Figure 2.2 Hysteresis loops and polarization of ferroelectric materials. [24]

2.1.2 Perovskite type structure

As aforementioned in topic 2.1.1, perovskite structure is an important structure which shows ferroelectric property and is widely used in many applications. Generally, perovskite compound structures have isomorphous structures with the perovskite ie. $CaTiO_3$. Fig. 2.3, shows the crystal structure of perovskite (ABO_3). In general, the chemical formula ABO_3 stands for the element sites of the perovskite structure unit, the site of A and B are cations and O is oxygen site.

ลิขสิทธิ์มหาวิทยาลัยเชียงใหม่
Copyright© by Chiang Mai University
All rights reserved

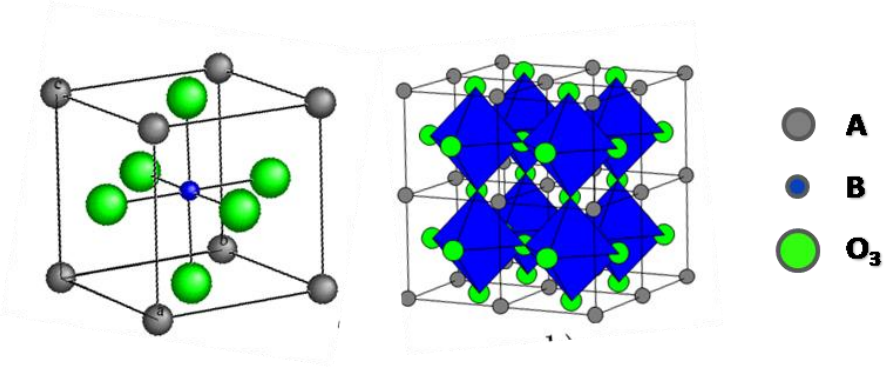

Figure 2.3 The perovskite crystal structure [20].

From Fig. 2.3, perovskite structure has the strong construction of BO_6 octrahedra inside the A cation framework. The BO_6 octahedra links with another one by sharing face site of O-site and corner site of A-site. However, this type of structure is a very tolerant one and suitable to adapt with many different ions. This gives a large number of occupant oxides. The stable perovskite structure has balancing valencies of the ions and the ionic radii meet the Goldschmidt criteria as defined in equation (4.1) [25].

$$t = \frac{r_A - r_o}{\sqrt{2}\,(r_B - r_o)} \tag{4.1}$$

where r_A r_B and r_o are the ionic radius of the A, B and O cations. The ideal model of cubic perovskite structure should possess t = 1. The structure is stable with 0.85 < t < 1.05. A list of ions that generally form perovskite, is given in Table 2.2.

From Table 2.2, the cubic structure can be estimated from tolerance factor that equal to 1. However, the perovskites which have less than 1 of tolerance factor meaning that there are the distortion in their structures and will become ferroelectric materials. Examples of some perovskite with their tolerance factors are shown in Table 2.3.

Table 2.3 shows the tolerance factor and the properties of perovskite oxide, which is ferroelectric material. These interesting perovskite oxide groups are frequently available in many applications. One of the best examples is BT. BT is cubic above 135°C, and then changes to a tetragonal (ferroelectric

ลิขสิทธิ์มหาวิทยาลัยเชียงใหม่
Copyright© by Chiang Mai University
All rights reserved

structure) at lower temperature. Recently researches have reviewed the change of BT perovskite structure which are shortly summarized here. The Ba and Ti ions are moved involving to the anion extent along one of the cubic <001> directions. The polar axis possibly has six ways of directions in the tetragonal phase. At about 5°C the second phase transition occurs, from the tetragonal → orthorhombic phase, while the polarization appears owing to the move of cations along one of the cubic <110> directions. Lastly, at about −90°C the transition of orthorhombic to rhombohedral phase occurs with the cations being moved along one of the cubic <111> directions.

Table 2.2 Lists of cations regularly formed perovskite-structured oxides with the ionic radius [23].

A-site Cation	Ionic radius when [12][a] by O^{2-}(Å)	B-site Cation	Ionic radius when [6][b] by O^{2-}(Å)
Na^{+}	1.32	Nb^{5+}	0.64
K^{+}	1.6	Ta^{5+}	0.68
Ba^{2+}	1.6	Zr^{4+}	0.72
Sr^{2+}	1.44	Ti^{4+}	0.605
Pb^{2+}	1.49	Pb^{4+}	0.775
Bi^{3+}	1.11	Sc^{3+}	0.73
Ca^{2+}	1.35	Fe^{3+}	0.645

a"12-fold coordinated", **b**"6-fold coordinated"

Table 2.3 The tolerance factors of some perovskite and their properties [23].

Perovskite oxide	Tolerance factor	Structure at 20°C	Type	T_C (°C)
$BaTiO_3$	1.06	Tetragonal	Ferroelectric	135
$SrTiO_3$	1.00	Cubic	Paraelectric	-
$CaTiO_3$	0.97	Tetragonal	Paraelectric	-
$PbTiO_3$	1.02	Tetragonal	Ferroelectric	490
$NaNbO_3$	0.94	Monoclinic	Ferroelectric	−200
$KNbO_3$	1.04	Tetragonal	Ferroelectric	412

ลิขสิทธิ์มหาวิทยาลัยเชียงใหม่

2.1.3) Potassium sodium niobate

Sodium potassium niobate or KNN is one of the most interested lead-free ferroelectric systems with perovskite structure. The beginning of KNN research started in the early 1950s -1960s, while the intensive investigation started in the late 1990s due to the increase of environmental awareness from lead-mixed component. KNN is well known as lead-free material which has a high Curie temperature (T_c) and high piezoelectric (d_{33}) values of the same order of magnitude. Even if, the dielectric constant (ε_r) of KNN is not as high as that of lead-based materials like PZT, but it's low dielectric constant with high electromechanical coupling coefficient (k_p), make this material interested for ultrasonic device [26]. The compositions that is shown highest k_p is the nearest morphotropic phase boundary (MPB) at 52.5 mole% of $NaNbO_3$, lead to intensive studies in composition of $(K_{0.5}Na_{0.5})NbO_3$ and subsequently referred to KNN [9,11-12,27].

Although, KNN compound is of interest in the wide researches, but, there are some problems with KNN that affect to manufacturing process. KNN materials are normally prepared from alkaline carbonate compound via conventional mixed oxide technique, which is an easy and simple method. Alkaline carbonate is often used as law material due to their low cost. However, the alkaline carbonate compounds are usually known that it is easy to volatile at room atmosphere. This needs to be carefully controlled of the moisture, pressure and temperature in manufacturing process [28]. Furthermore, the high temperature using in sintering ceramics process initiates the volatility of potassium and causes the lower ceramics densification and possibly a change in phase composition. Thus, it is so difficult to form $(K_{0.5}Na_{0.5})NbO_3$ morphotropic phase compound.

KNN is a solid solution between orthorhombic ferroelectric potassium niobate (KN) and orthorhombic anti-ferroelectric sodium niobate (NN). The first report of KN-NN solid solution as a ferroelectric system was done in 1954 by Shirene et al. [27]. The dielectric, structural and optical properties of NN and KNN ceramic and single crystal have been carried out. Here, they

ลิขสิทธิ์มหาวิทยาลัยเชียงใหม่
Copyright© by Chiang Mai University
All rights reserved

found ferroelectric property of a small addition of KN to NN. They did not report the effect of increasing 50% potassium and 50%sodium ratio. Then, in 1959, Egerton et al. [9] reported the piezoelectric data in KNN compound. Their report showed that the increasing of KN and NN up to 50:50 by mole is also enhanced ferroelectric property of KNN compound.

Before getting to know about KNN solid solution, the data information of KN and NN should be firstly studied for better understand the KNN phenomenon. There are a few study which was reported KN and NN characteristics. In 1971, Jaffe et al. [12] had reported the psuedobinary phase diagram (Fig. 2.4) between KN and NN. The report showed the behavior of KN and NN single phase during temperature changing. At room temperature, KN structure is orthorhombic. At lower temperature ($< -12°C$) KN is rhombohedral. When heating KN up to 225°C, their structure is changed from orthorhombic to tetragonal and then the high temperature at about 435°C also changes tetragonal phase to cubic phase. While, the cubic phase in NN has higher temperature than that found in KN at 630°C. Anyway, NN phase transitions at lower temperature are undergoes a sequence of phase transitions and is anti-ferroelectric at room temperature.

From Fig. 2.4, the phase diagram of KN-NN is summarized in many literatures [12,28-29]. In binary phase diagram of KN-NN, it can be seen that at room temperature, all of KN-NN compositions show orthorhombic perovskite structure. The symbolize from Fig. 2.4 can be describe as followed; F_R–ferroelectric rhombohedral with high potassium, F_{MONO}–ferroelectric monoclinic, F_{O1}–ferroelectric orthorhombic, F_{O2}–ferroelectric orthorhombic, F_{OM1}–ferroelectric orthorhombic field enforced in pure $NaNbO_3$, F_{OM2}–ferroelectric orthorhombic, F_{T1}–ferroelectric tetragonal with high potassium, F_{T2}–ferroelectric tetragonal, F_{TM}–ferroelectric tetragonal obtained with additives, A_O–antiferroelectric orthorhombic, P_C–paraelectric cubic, P_{OM}–paraelectric orthorhombic, P_{TM}–paraelectric tetragonal, P_{TM2}–paraelectric pseudotetragonal, P_{TM3}–paraelectric pseudotetragonal. The morphotropic phase boundaries of this binary system located at around 52.5,

ลิขสิทธิ์มหาวิทยาลัยเชียงใหม่
Copyright© by Chiang Mai University
All rights reserved

67.5, 82.5 and 98.0 mole% of NN, divided the 2 different orthorhombic phases, respectively. In 1968, Tennery et al. [28] also suggested that this solid solution shows a monoclinic with a very little distortion in tenths of degree.

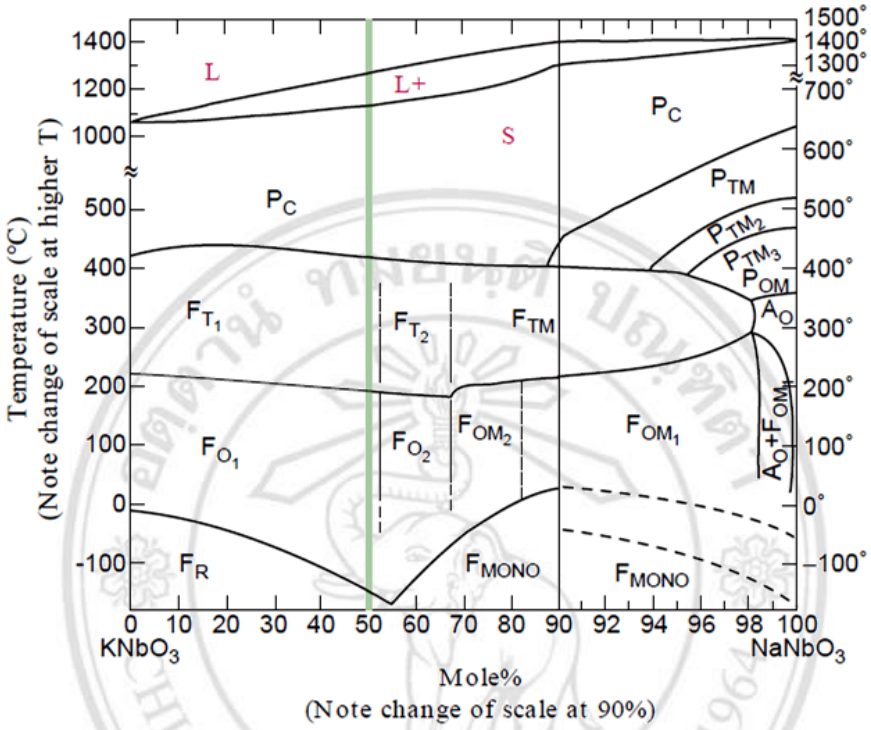

Figure 2.4 Binary phase diagram $KNbO_3$–$NaNbO_3$ [12].

The characteristic of KNN has been explained in many works. However, phase diagram of KNN has not been completely reviewed, according to the JCPDS data which shows no specific composition of $(K_{0.5}Na_{0.5})NbO_3$. Thus, the $(K_{0.5}Na_{0.5})NbO_3$ composition is referring to the phase diagram, isostructural with $KNbO_3$ (Bmm2, a=0.5697nm, b=0.3971nm, c=0.5721nm) [30].

From thermal and XRD analysis, the Curie temperature (T_c) of $K_{0.5}Na_{0.5}NbO_3$ is approximately 400ºC, which means that KNN materials in composition of $K_{0.5}Na_{0.5}NbO_3$ are well used in high temperature. In temperature range of 200ºC - 400ºC, $K_{0.5}Na_{0.5}NbO_3$ structure is tetragonal. Upon cooling down from 200ºC to −160ºC, the tetragonal phase transforms to orthorhombic phase, and below −160ºC, the orthorhombic phase transforms to a rhombohedral phase as shown in Fig. 2.5. The melting points (melting

ลิขสิทธิ์มหาวิทยาลัยเชียงใหม่
Copyright© by Chiang Mai University
All rights reserved

temperature; T_m) of $KNbO_3$ and $NaNbO_3$ are at 1,040 ºC and 1,420 ºC, respectively. For $K_{0.5}Na_{0.5}NbO_3$, the T_m is at about 1,280 ºC.

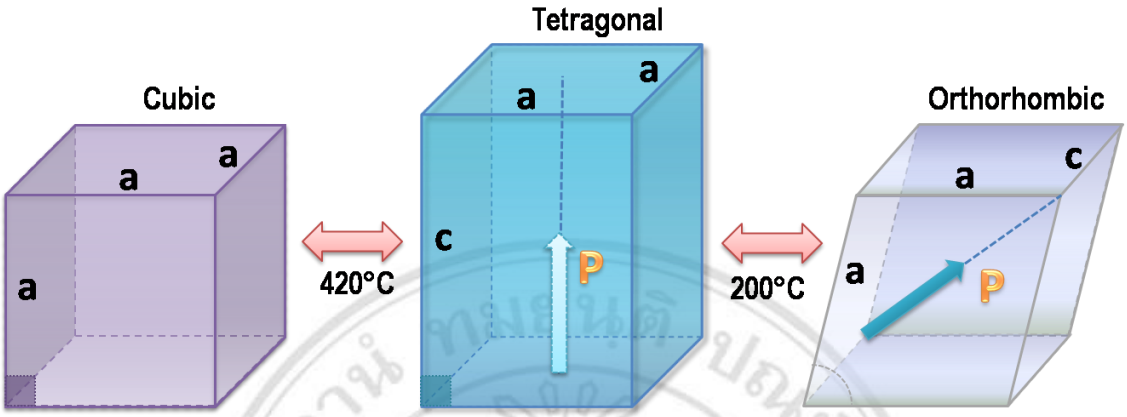

Figure 2.5 The transformation of KNN crystal structure at different temperature [11]. Here P stands for the direction of polarization.

There are many research works studied the binary phase diagrams of K_2O-Nb_2O_5 and Na_2O-Nb_2O_5. The binary phase diagram of K_2CO_3–Nb_2O_5 with an incongruent melting temperature of about 1,039ºC showed KNb_3O_8, K_3NbO_7, $K_4Nb_6O_{17}$ and $K_6Nb_{44}O_{113}$ phases [31]. The studies of the niobium-rich region (Nb_2O_5) in $KNbO_3$ also revealed $K_{5.75}Nb_{10.85}O_{30}$, $K_3Nb_7O_{19}$, $K_2Nb_8O_{21}$, KNb_7O_{18}, and $KNb_{13}O_{33}$ [32-33]. Normally, the stoichiometric $KNbO_3$ is stable. However, the slight substoichiometry of potassium component causes to the separation in phases, one of them is strongly hygroscopic [34]. As reported by Bizeto's work [35], $K_4Nb_6O_{17}$ composition is easily formed stable hydrates, with water molecules intercalated in its layered structure. The binary phase diagram of Na_2O–Nb_2O_5 was completely studied since 1959 [36], sodium niobate composition contains five phase patterns as $NaNbO_3$, $NaNb_7O_{18}$, $NaNb_{10}O_{25}$, $Na_2Nb_8O_{21}$ and Na_3NbO_4. The phase diagrams of the Nb_2O_5-rich phase in $NaNbO_3$ system contain the different sodium niobate phases as $Na_2Nb_4O_{11}$, $Na_{1\pm x}Nb_{3\pm x}O_{8\pm 2x}$, $Na_2Nb_{12}O_{31}$, $NaNb_7O_{18}$, and $NaNb_{13}O_{33}$ as well as $NaNbO_3$ [32-33].

ลิขสิทธิ์มหาวิทยาลัยเชียงใหม่
Copyright© by Chiang Mai University
All rights reserved

As present, the Nb_2O_5-rich phase has an effect to KNN stoichiometric in the individual K_2O–Nb_2O_5 and Na_2O–Nb_2O_5 phase diagrams. The occurances of Nb_2O_5-rich phase attribute to the high hygroscopicity of the alkaline carbonates, especially potassium carbonate, and also the volatility of carbonate during firing at high temperature of about 700ºC to 950ºC. Thus, it can be expected that polyniobate phases are formed in the ternary Na_2O–K_2O–Nb_2O_5 system.

S.J. Zhang et al. [37] have compared KNN properties with other materials in 2007. The room temperature values of dielectric and piezoelectric are plotted as a function of T_c as shown in Fig. 2.6. The dielectric and piezoelectric properties are increased with decreasing in T_c for PZT-based materials. The comparisons of the electrical properties between current major lead-free systems and PZT are listed in Table 2.4.

In Table 2.5, several techniques were used for improving the fabrication process and the property of KNN ceramics, i.e. hot pressing technique, crystallographic texturing, sintering aid, etc. In 1962, Jaeger et al. [11] reported that hot pressing techniques (HP) was used to prepared KNN ceramics with increased the ceramic density from 4.25 g/cm^3 (by conventional mixed oxide method) to 4.46 g/cm^3 (by HP). Their research also increased d_{33} of this material from 80 pC/N to 160 pC/N. Recently, the use of sintering aids was subjected to intensive studies to the possibility improve the KNN ceramic properties. The sintering aids mainly used in many works are copper-based like CuO [40-41], $K_4CuNb_8O_{23}$ [42-43] and $K_{5.4}Cu_{1.3}Ta_{10}O_{29}$ [44-45]. The results in adding copper-based materials as a sintering aid are the improvement of the KNN ceramics density. Other techniques that used for improving KNN ceramics are included cold isostatic pressing (CIP). However, CIP techniques are good to improve the density of green compacts but cannot improve dielectric and piezoelectric properties.

To improve the piezoelectric performance of $Na_{0.5}K_{0.5}NbO_3$, the other material was added to make solid solution and form complex perovskite structure within this material, by aimed at creating MPB phase which showed

ลิขสิทธิ์มหาวิทยาลัยเชียงใหม่
Copyright© by Chiang Mai University
All rights reserved

high piezoelectric property. The solid solutions of KNN with other additions have been already reported including; KNN-$SrTiO_3$ [46-48], KNN-$(Bi_{0.5}K_{0.5})TiO_3$ [49], KNN-$BaTiO_3$ [50-51], KNN-$LiTaO_3$ [39,52-54], KNN-$LiNbO_3$ [55-59] and KNN-$LiSbO_3$ [60-62]. Besides, the highest piezoelectric of about 416 pC/N was found in KNN added Li-Ta-Sb system in Saito's work in 2004 [39].

Lately, a new technique of template grain growth (TGG) is subjected to intensive studiesd, in order to have a desirable KNN ceramic properties. TGG technique is involves the fabrication of the template, tape casting and stacking tapes to make green compact.

Table 2.4 Electrical properties of lead-free systems vs PZT [37].

	Perovskite structure ferroelectric			
	$BaTiO_3$ [12]	**$(Bi_{1/2}Na_{1/2})TiO_3$ [37]**	**$(Na_{0.5}K_{0.5})NbO$ [9,11,24]**	**PZT [12]**
Curie temperature; T_c (ºC)	120	320	420	300~400
d_{33} (pC/N)	190	120~200	100~416	200~500
d_{31} (pC/N)	-78	-7.5	-30~-152	-130
Dielectric constant (1kHz)	1500~6000	~1700	200~500	1000~4000

Table 2.5 Dielectric and piezoelectric properties of lead free KNN based ceramic systems.

KNN-based compound	**ε/ε0**	**tanδ**	**d_{33} (pC/N)**	**k_p**	**T_c (°C)**	**Reference**
KNN	290	0.04	80	0.35	420	**[9]**
KNN (HP)	420	0.035	160	0.46	420	**[11]**
KNN-Li-Sb-Ta	1570	-	416	0.61	253	**[39]**
KNN-$LiTaO_3$ (5%)	570	0.04	200	0.36	430	**[52]**
KNN-$LiNbO_3$ (5%)	-	-	230	0.44	460	**[55]**
KNN-$SrTiO_3$ (5%)	950	-	200	0.37	277	**[47]**
KNN-$(Bi_{0.5}K_{0.5})TiO_3$ (3%)	850	0.04	192	0.45	370	**[49]**
KNN-$BaTiO_3$ (2%)	1000	0.04	104	0.295	358	**[50]**
KNN-$LiSbO_3$ (5%)	1288	0.019	283	0.50	392	**[60]**

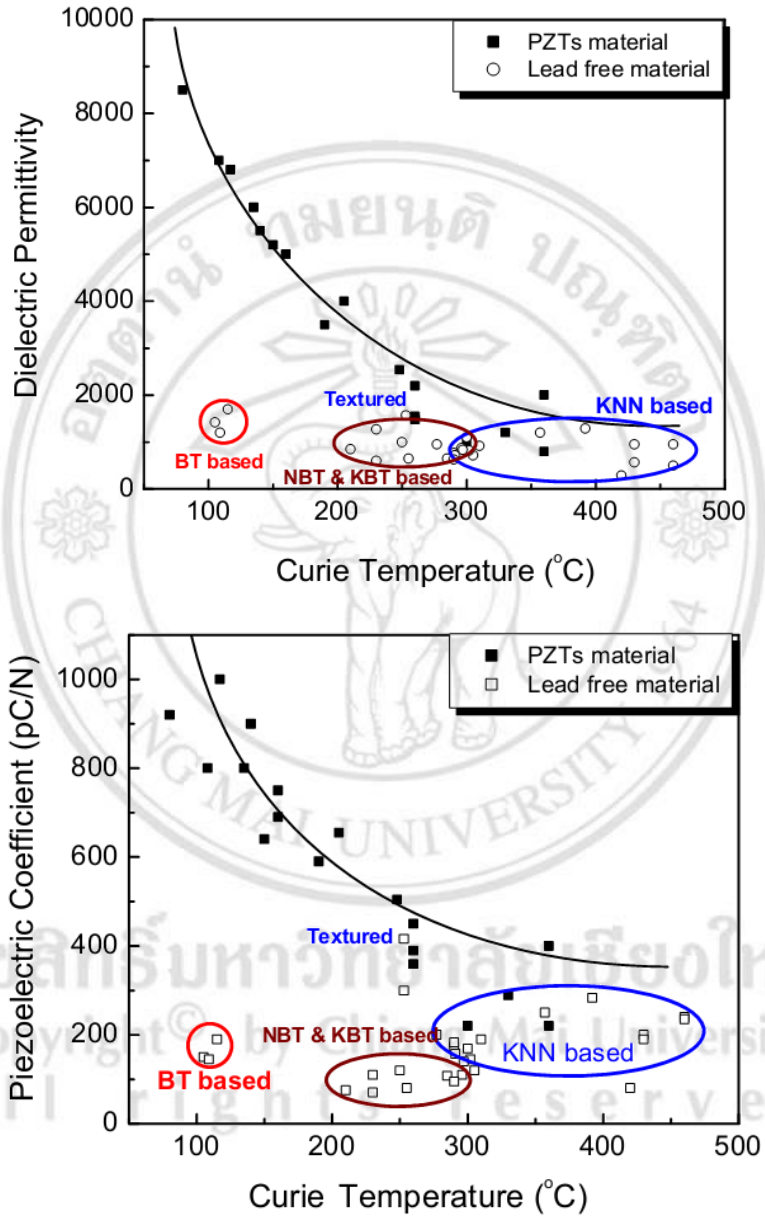

Figure 2.6 The comparison between KNN based ceramics and other materials. [37]

(a.) dielectric permittivity as a function of Curie temperature,

(b) piezoelectric coefficient as a function of temperature.

ลิขสิทธิ์มหาวิทยาลัยเชียงใหม่
Copyright© by Chiang Mai University
All rights reserved

2.2 Glass-ceramics

Glass-ceramics was first discovered in mid-1950s by Stanley Donald Stookey [4], the famous glass chemistry from Corning Glass works. Stookey accidentally found glass-ceramics due to the need in precipitating silver particles in lithium disilicate glass for making a permanent photographic image. To precipitate silver particles, he started to heat glass at above glass transition temperature (450˚C). He surprised that glass with accidentally over-heated to 850˚C showed white material instead of melted pool glass. After studied glass composition, he found that its structure does not change from glass, and it is also stronger than normal glass. This made him realized that he found new ceramics-material and called it glass-ceramics (Trade mark of first glass-ceramics; FOTOCERAM™ later name PYROCERAM™). Since then, many research works have been reported and patent granted related to glass-ceramics by research institutes, universities and industrials in worldwide.

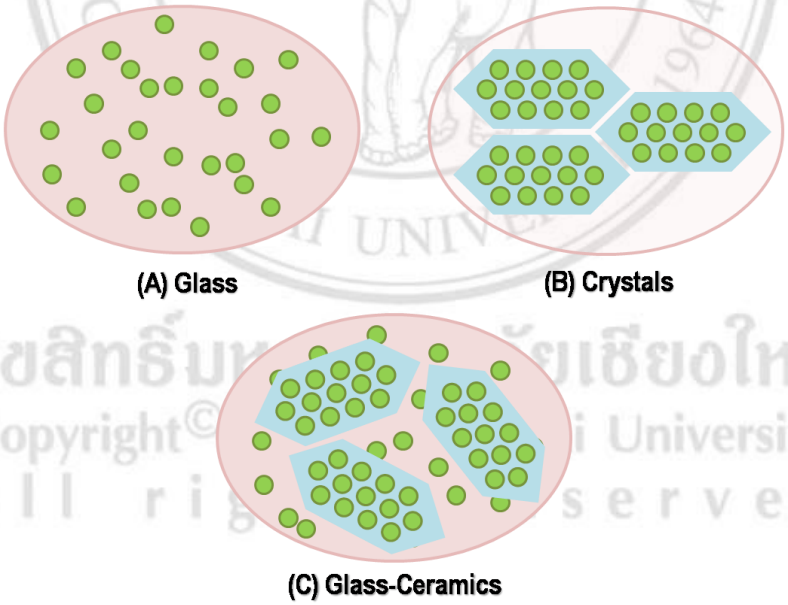

Figure 2.7 Schematic images of **(A)** glass, **(B)** crystal, and **(C)** glass-ceramic [63].

ลิขสิทธิ์มหาวิทยาลัยเชียงใหม่
Copyright© by Chiang Mai University
All rights reserved

Glass-ceramics are materials in which incorporate the properties of glass and ceramic together. The advantages of glass-ceramics when compared with conventional ceramics are the uniformity of microstructure, the ability of reproduction, and the flexibility of fabrication during glassy state. Glass-ceramics are unlike glass and ceramic. Glass-ceramics compose glass matrix and ceramic crystals. The degree of crystallinity varies from 0.5% to 99.5%, but they are frequency found to lie between 30% and 70% [64]. The schematic images (Fig. 2.7) are briefly descript the different between glass, ceramic and glass-ceramics.

Glass-ceramics have less porosity or free from porosity, unlike ceramics, but sometimes, they have a little possibility in occurrence of bubbles during the crystallization process. Glass-ceramics have more advantages such as the ability to produce in mass production and design nanostructure or microstructure as required applications. Lately, many works reported that glass-ceramics showed a wide range of thermal shock or thermal expansion and high mechanical strength with zero porosity. Those interesting advantages also combine the transparency in visible region. So, these marvelous properties raised glass-ceramics to be used in many devices since architectural materials to warehouse materials to biomedical materials as dental applications and bone implants. The favorable characteristics of glass-ceramics have been once summarized by Holand and Beall [4] and listed in Table 2.6.

The commercial glass-ceramic products are available in many fileds since 1950s. The first commercial glass-ceramics was used in aerospace industry for military as radomes, the cover of nosecones for aircrafts and rockets. The year after, glass-ceramics become well known materials worldwide for examples: the kitchen utensil as cooking wares, cooktop plates: the construction materials as marble or granite-like floor and wall tiles: the bioactive materials as Cerabone A-W for bone replacement etc.: the electrical insulating and conducting glass-ceramics for electronic parts: glass-ceramics armor as bullet-proof vests and armor for automobile, aircraft, helicopter etc. Thus, this available application is informed us that glass-ceramics can be develop for more applications. The variation in glass-ceramic compositions give us a chance for finding new glass-ceramics with extraordinary properties.

ลิขสิทธิ์มหาวิทยาลัยเชียงใหม่
Copyright© by Chiang Mai University
All rights reserved

Table 2.6 The summarization of favorable properties of glass-ceramics [4].

Particularly favorable properties of glass-ceramics
Processing properties
• Via rolling, casting, pressing, spinning, press-and-blow, drawing and etc. without shrinkage and porosity
Thermal properties
• With low expansion nearly zero and with high thermal stability
Optical properties
• Transparency to opacity, pigment variation, opalescence and fluorescence
Chemical properties
• Resorbability or high chemical durability
Biological properties
• Biocompatibility and bioactivity
Mechanical properties
• Machinability, high strength and toughness
Electrical and magnetic properties
• Isolation capability (low ε_r, $tan\delta$, high resistivity and break down voltage), Ion conductivity and superconductivity, Ferromagnetism

Moreover, the technologies of glass-ceramics are subjected to intensive studies due to the wide varieties in preparing process [64]. The aim of preparation technology is to design the glass-ceramic properties by controlling the nucleation and the crystallization of glass. Moreover, an additive crystal can be a nucleating agent for glass batch for desired microstructure and property in glass matrix. Generally, glass-ceramics are produced in 2 steps, firstly, the forming glass, secondly, the shaping, cooling and reheating above glass transition temperature. In the reheat or heat treatment process, glass samples partly crystallizes inside glass matrix, and here, the nucleating agent is significant factor for boosting up the nucleation process. Fig. 2.8 shows the basically explanation to glass-ceramics process that relevant to heat treatment temperature.

ลิขสิทธิ์มหาวิทยาลัยเชียงใหม่
Copyright© by Chiang Mai University
All rights reserved

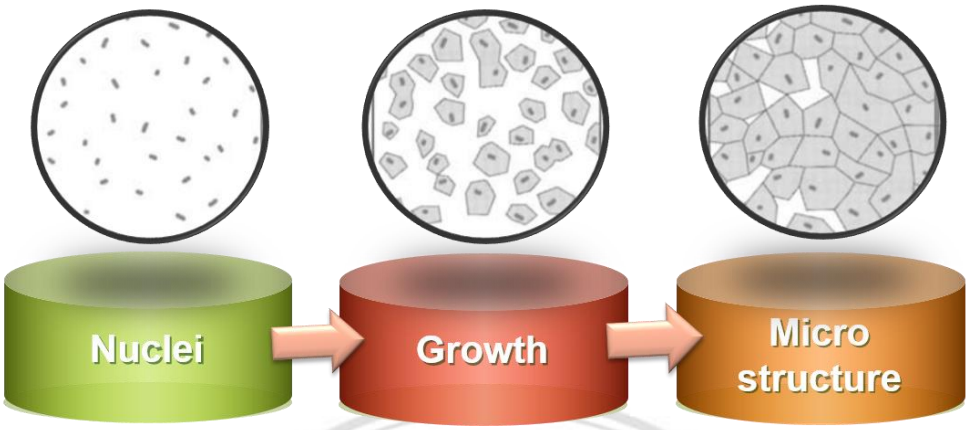

Figure 2.8 Glass-ceramic mechanism during heat treatment process.
(a) Nuclei formation, **(b)** nuclei growth and **(c)** crystal structure in glass matrix. [4]

More techniques in glass-ceramic preparation were introduced [64]. A less interesting technique is induction and control internal crystallization process during cooling glass melt which often form the coarse-grain glass-ceramics. This techniques are used in the construction industry. Another technique which often used is sinter-crystallization of glass powder [4,64]. The glass powder were pressed as required shape and then sintered at the proper temperature. The sintering techniques of compacted glass powder starts the crystallization process at the interfaces of glass particle. In this techniques, the nucleating agent is not necessary because the glass particles act like nucleation site. However, compacted glass powder leaves the void or porosity of about 0.5% – 3.0%. Thus, new fabrication techniques such as hot-pressing were introduced to reduce the chance of pore occurrence during sintering process. The examples of glass application which used sinter-crystallization are solder glasses for sealing TV tubes, cofired multilayer substrates for electronic packaging, marble like floor and wall tile and bioactive glass-ceramics.

2.2.1) Theory of glass and glass-ceramics

There are different types of material divided by their properties. Glass is an enormous type of material groups that proposed high transparency with the ability in adjusting the chemical composition. Glass has no grain boundary, that similar to a characteristic of liquid, achieved high transparency of glass makes it to be a fundamental material for our daily life, i.e., optical glass

ลิขสิทธิ์มหาวิทยาลัยเชียงใหม่
Copyright© by Chiang Mai University
All rights reserved

fibres, window and display panel glass. In addition, glass material also shows good formability, which is originated from the random network structure with interstitial free volume. Thus, this large and long glassy material can be effortless prepared than those of inorganic crystal.

In Fig. 2.9, it can be seen that glass consists of a short-range in order of atoms that can be form in various coordination polyhedral structure. It is called an amorphous structure [65]. The amorphous structure is unlike crystal structure, as ceramics and other materials which have the long range ordering bond. On the other hand, the random network of glass closely correlates with the chemical composition diversity, which in turn allows us to tailor physical property and various functionalities. The diversity is also a unique characteristic of amorphous glass materials. There are many definitions of glass which has been reviewed in many works. The most conventional definition of glass is descripted by ASTM standard as “Glass is an inorganic product which is melting and quenching into rigid condition without crystallization” [66]. It can be seen that glass formation can be form the solid material which is melted at high temperature and immediately quenched to lower temperature.

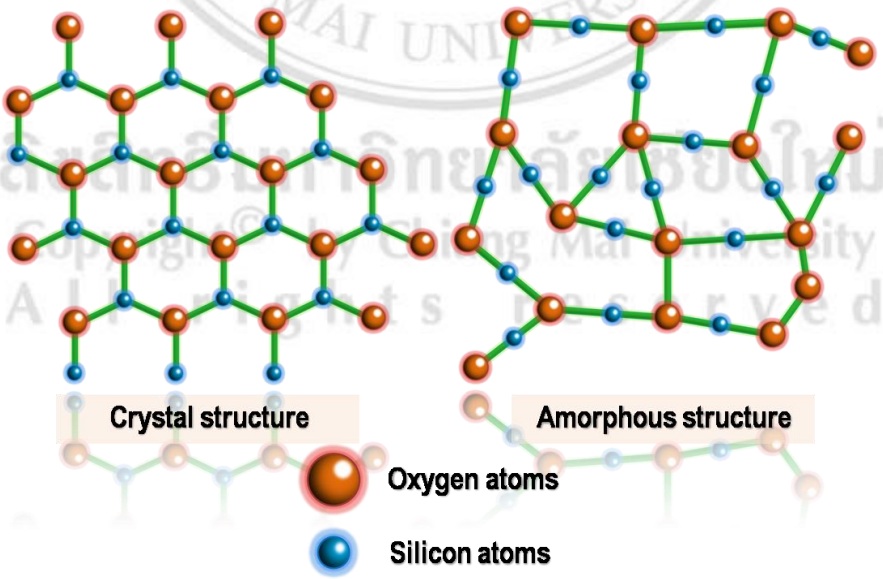

Figure 2.9 The comparative illustrate between crystal type structure and amorphous type structure of silicate glass [67,68].

Fig. 2.10 shows the effect of cooling rate in quenching glass liquid process. The fast and slow cooling rate effect to glass in different way. The slow cooling rate process allows enough time to decrease temperature, thus the atoms can rearrangement and form crystal structure. While for the fast cooling rate process, the free moving atoms in liquid glass are blocked due to the rapid change of high temperature to lower temperature. Thus, the atoms are arranged in random disordering with glass characteristic.

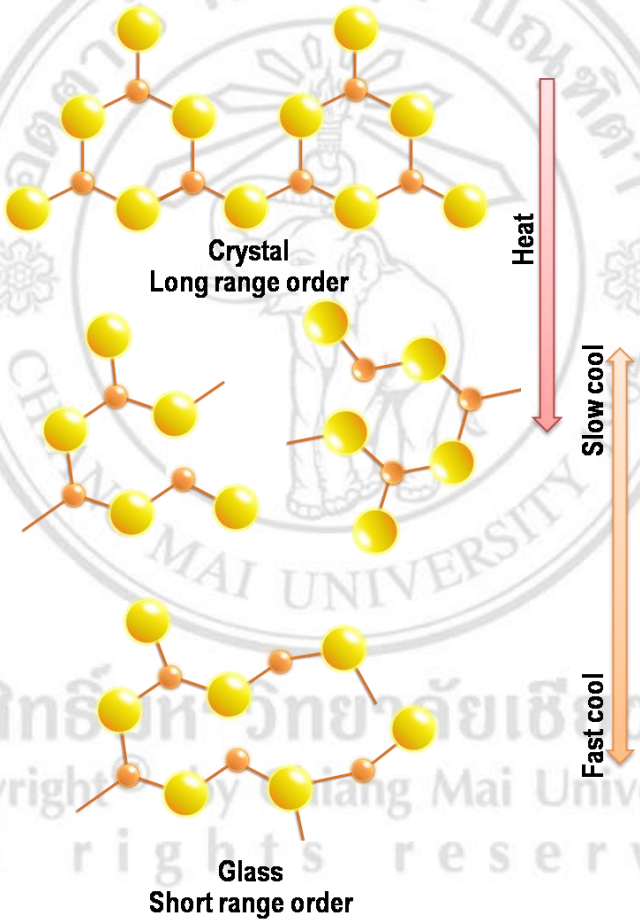

ลิขสิทธิ์มหาวิทยาลัยเชียงใหม่
Copyright© by Chiang Mai University
All rights reserved

Figure 2.10 The schematic diagram of atomic rearrangement of glass and crystal showing the effect of slow and fast cooling rate from liquid melt structure [67,68].

Besides, the explanation of the glass formation via enthalpy diagram was introduced. The enthalpy of glass and crystal are changed as a function of temperature as shown in Fig. 2.11. From Fig. 2.11, the relationship between these states by means of a volume-temperature diagram has been demonstrated [63,69]. This diagram can also be presented in terms of an enthalpy temperature because volume and enthalpy behave in a similar manner.

In general, the melt has a short-range structure characteristic of liquid. Under cooling process, the atomic structure of the melt will slowly change but still keep the characteristic of short-range order of the primary liquid. When the melt is cooled below the melting temperature (T_m), the small solid crystal occurs and it becomes solid. In contrast, a glass material goes though the super cooled state below the T_m, and exhibits the transition to glass in the temperature range at the viscosity of 10^{13} dPa·s. The temperature at this point is called as the glass transition temperature, T_g [63].

From diagram, the rapid decrease of enthalpy develop crystals. On continually cooling, the enthalpy will decrease slowly controlled by the heat capacity of the crystal. However, if the liquid can be cooled below the melting point by avoiding crystallization, there will be an undercooling of the melt to give a supercooled liquid. No discontinuous rearrangement happens in this case as the temperature decreases, the overall enthalpy gradual changes. Further cooling produces deviation from the equilibrium line since the viscosity of the melt greatly increases, inhibiting atom movement, leading to difficulty in the rearrangement of atoms in the equilibrium liquid structure. Then as the temperature decreases, the viscosity increases rapidly, resulting in frozen-in, liquid-like structure. The slope after this is determined by the heat capacity of the frozen liquid. The glass transformation region defined by the temperature region joining the equilibrium liquid state and the frozen liquid state. Hence, the frozen liquid is a glass [65,70]. In the temperature region, some physical parameters of glass material show “some steep”

ลิขสิทธิ์มหาวิทยาลัยเชียงใหม่
Copyright© by Chiang Mai University
All rights reserved

change. Since the T_g is a fictive temperature that depends on the fabrication process, a glass can take several values of T_g depending on the cooling rate.

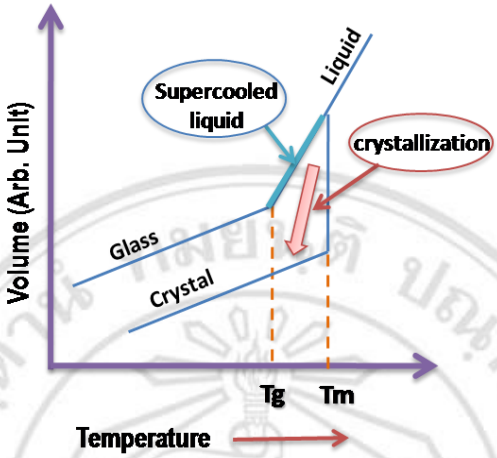

Figure 2.11 The volume change of glass and crystal compared with temperature [63].

As shown in Fig. 2.11, there is a volume difference between crystal and the glass, which originates from the free volume of glass material possessing the random network. Because of the random network structure, the Gibbs free energy of a glass material is inherently larger than that of the corresponding crystal, and glass materials exist as a metastable state. It means that phase transition of glass to crystalline phase can progress above the T_g, at which migration of the compositional units starts. The thermal transition process from glass to the corresponding crystal is called crystallization of glass. On the other hand, the resulting glassy material containing some precipitated crystallites is designated as a "glass-ceramic". Since the short-range ordering of glass is basically identical to that of crystal, the glass-ceramic can be said as a glassy material possessing partially long-range and/or medium-range ordering. Such glassy material containing both ordered and disordered parts is the main target of this chapter.

ลิขสิทธิ์มหาวิทยาลัยเชียงใหม่
Copyright © by Chiang Mai University
All rights reserved

2.2.2) Hypothesis of crystallization in glass-ceramics

Normally, the temperature above T_g is a driving force for metastable amorphous glass to transform to stable ordered crystal. In earlier years, crystallization of glass was called devitrification of glass, because there is a difference in refractive index between the precipitated crystallites and the residual amorphous regions. The formation of boundary within a matrix by crystallization often brings about a loss of transparency of the material due to the Mie scattering. To overcome this problem, two approaches can be used:

1) tuning the refractive index by addition of various kinds of oxides, and
2) controlling the size of precipitated crystallites.

The former approach is realized by using a database of optical property of glass matrix. Since the additivity between property and compositions usually holds in glass material, tailoring of refractive index can be attained empirically. On the other hand, the later approach is of importance even in a glass possessing the same chemical composition as the crystal, in that case the mismatch of refractive index between crystallites and residual amorphous is relatively small. As mention in Fig 2.11, crystallization from a supercooled liquid state above the *T*g progresses via two processes; i.e. nucleation and crystal growth. The rates of nucleation and crystal growth depend on the heat-treatment temperature as well as crystalline composition. Fig. 2.12 shows a schematic depiction of rates of nucleation and crystal growth in glass [63,71].

As shown in Fig. 2.12, the maximum rates of nucleation and crystal growth occur at different temperatures. In addition, nucleation preferentially occurs in the low-temperature region above the T_g. Precipitation of either large crystallites (> several μm) or small crystallites (< several nm) is effective for maintaining the transparency of the glass after crystallization. The latter crystallization, in which nano-sized crystallites are precipitated, is often referred to as "nano-crystallization". In the case of precipitation of crystallites from the glass matrix that possesses chemical composition different from the stoichiometric composition of crystal, the nano-crystallization process is

ลิขสิทธิ์มหาวิทยาลัยเชียงใหม่
Copyright© by Chiang Mai University
All rights reserved

quite of importance. Glass-ceramic, which is usually obtained by heat-treatment, *i.e.* crystallization, of a precursor glass, is a kind of glassy material consisting of disordered glass regions and ordered precipitated crystalline regions. Since glass-ceramic permanently shows both glassy and crystalline characteristics without any temporal change below the *T*g, it may be mentioned that glass-ceramic is an inorganic composite material possessing not only merits of glass materials but also its unique physical properties of the corresponding crystals.

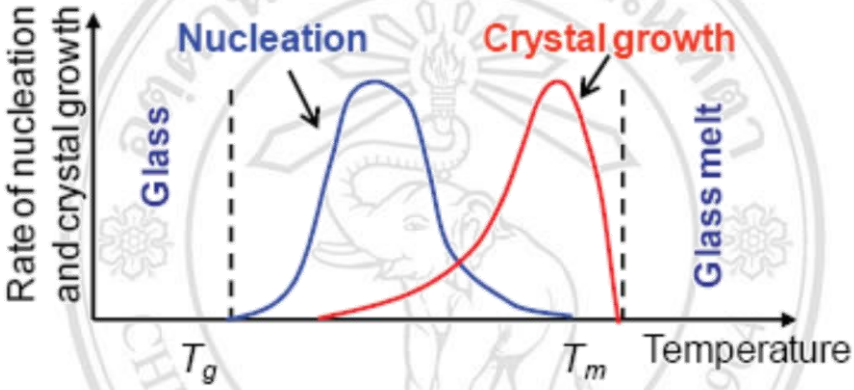

Figure 2.12 Schematic depiction of rates of nucleation and crystal growth in glass [63].

The crystallization or devitrification is very important in the glass-ceramic process. This process must be controlled in order to have the correct microstructure and properties of final materials [72,73]. Crystallization is the consequence of two individual kinetic processes, which are nucleation and crystal growth. In terms of nucleation, two contributions concerned with the stability of a particle in homogeneous nucleation are the free energy and the interfacial energy. At the melting point, the free energy of a material is the same in both the crystalline and liquid forms. The melt of a single element is cooled below the melting point, the crystalline form will have a lower free energy and, if nuclei available, the liquid will crystallize. The following equation shows the free energy change for the nucleation.

$$\Delta G = -\frac{4}{3}\pi r^3 \cdot \overline{\Delta G} + 4\pi r^2 \sigma \qquad (2.1)$$

ลิขสิทธิ์มหาวิทยาลัยเชียงใหม่
Copyright© by Chiang Mai University
All rights reserved

Where each terms mean,

ΔG the change in free energy per unit volume for the crystal-liquid transformation.

$\frac{4}{3}\pi r^3$ the volume of the nucleus (r is the radius of nucleus or crystal)

σ the surface tension or interfacial energy and

$4\pi r^2$ the surface area.

The critical radius (r^*) can be defined by $r^* = \frac{2\sigma}{\Delta G}$, where $\frac{d(\Delta G)}{dr}$. If particles have a radius smaller than r^*, they are called embryos, $\frac{d^2(\Delta G)}{dr^2}$ is positive and thus they are unstable. On the other hand, if they have radius greater than r^*, they are called nuclei, $\frac{d^2(\Delta G)}{dr^2}$ is negative and therefore they are stable.

The rate of nucleation is controlled by the production of critical sized nuclei per unit volume and the rate at which atoms attach to the embryo. It can be shown in this following equation:

$$I = \left[N_S \frac{kT}{h} \exp\left(-\frac{\Delta G_a}{kT}\right)\right] \cdot \left[N \exp\left(-\frac{\Delta G^*}{kT}\right)\right] \quad (2.2)$$

N_s the number of atoms adjacent to the surface of embryos

h Planck's constant

$\frac{kT}{h}$ the vibrational frequency of the atom

ΔG_a the kinetic barrier to nucleation

ลิขสิทธิ์มหาวิทยาลัยเชียงใหม่
Copyright© by Chiang Mai University
All rights reserved

The first term is the number of atoms crossing the interface per second. In other words, the first term corresponds to the diffusion of matter during the formation of the nucleus by Turnbull and Cohen [74]. The second term is the probability of forming a nucleus larger than the critical size at the temperature, where N is the number of atoms per unit volume and ΔG^* is the thermodynamic barrier to nucleation. In terms of crystal growth, the rate of crystal growth is the rate at which atoms arrive and remain at the surface of the nucleus. The growth rate of the crystal (u) is given as follows:

$$u = \left[\lambda \upsilon_0 \exp\left(-\frac{\Delta G_a}{kT}\right)\right] \cdot \left[1 - \exp\left(-\frac{\Delta G}{RT}\right)\right] \quad (2.3)$$

λ the average interatomic spacing between atoms in the liquid and nucleus (crystal)

υ_0 the frequency at which the atom in the liquid vibrates due to thermal energy

ΔG_a the activation energy for an atom in the liquid to pass through the interface between the crystal and surrounding liquid

R the gas constant and

ΔG the energy change when an atom crosses the interface to the crystal

The first term gives the probability of an atom having sufficient thermal energy to leave the liquid and join the nucleus. The second term is the factor, which is formed by the consolidation of the reduction in energy when the atom has crossed the interface to the crystal [75].

The rates of homogeneous nucleation and crystal growth in a viscous liquid are shown in Fig. 2.12. From this figure, it can be noticed that, at the temperature at which the maximum nucleation rate takes places, the maximum possible number of crystal nuclei will be produced in a given length of time. Therefore, the optimum nucleation temperature (T_n) can be selected for the production of glass-ceramics.

2.2.3) Transparent ferroelectric glass-ceramics (TFGCs) [1]

Recently, many attention has been paid to TFGCs, due to its interesting property. They combine the low cost of fabrication and forming of transparent glass with the superior nonlinear optical and electro-optical properties of ferroelectric crystals. A successful fabrication of TFGC requires the nucleation and growth of crystallites that are too small to scatter light, yet large enough to have ferroelectric response. Later studies have demonstrated successful fabrication of TFGCs with compositions based on high refractive index glass matrix (e.g. tellurites containing ferroelectric $LiNbO_3$), or the

ลิขสิทธิ์มหาวิทยาลัยเชียงใหม่
Copyright© by Chiang Mai University
All rights reserved

ferroelectric oxides that form glass easily and then crystallize congruently (e.g. $LaBGeO_5$). Surface crystallization dominates the devitrification of these compositions. Strong second harmonic generation of light has been observed in a number of glass-ceramic systems, which makes them attractive for applications but so far the ferroelectric behavior has been demonstrated for very few systems.

Glass-ceramics have been developed for over forty years and numerous commercial products have been developed using this technology. Typically, based glass is prepared by the usual melt-quenching method; it is then formed in desired shape and size. Subsequently, the product is subjected to a two-step heat treatment at temperatures of maximum nucleation and controlled growth to yield desired microstructure. So, one might expects that the fabrication of TFGCs would be relatively straight forward. However, unlike conventional glass-ceramics there are additional requirements and complications that make the fabrication of TFGCs nontrivial. So, for photonic applications, a TFGC material should have: (a) high transparency obviously, (b) high optical nonlinearity including second harmonic generation, which requires high volume fraction of the ferroelectric phase, (c) alignment of active crystallites so that the optical response can be controlled electrically, and (d) ability to make films, fibers or other shapes as a glass that can be subsequently transformed into desired glass-ceramic microstructure. As we shall find, TFGCs have been prepared demonstrating the proof of concept for each of these qualities separately, but not in the same material that would be commercially acceptable.

ลิขสิทธิ์มหาวิทยาลัยเชียงใหม่
Copyright© by Chiang Mai University
All rights reserved

2.2.4) Material systems

The concept of TFGCs was initially developed at Corning in the mid 1960's to take advantage of the unique and useful properties of ferroelectrics, and convenient, controlled processing of glass-ceramics [8,76-77]. The melts of common ferroelectric ceramics do not form glass easily upon cooling; they need to be mixed with glass forming oxides in sufficient amount to suppress crystallization and stabilize the glassy state. Therefore, in general, a TFGC

material system will consist of a glass forming oxide and a FE oxide, which should be compatible enough to satisfy the four requirements mentioned above. The initial proof of concept was demonstrated for a few SiO_2 based systems in which a ferroelectric oxide (such as $BaTiO_3$, $LiNbO_3$, etc.) was dissolved and subsequently precipitated out by controlled devitrification. The briefly explain of silicate glass or SiO_2 properties can be seen in subtopic 2. The transparency of the glass-ceramic was retained so long as the crystallites were of sub-micron size (<200 nm). The particle size was large enough to exhibit FE-like behavior. This interesting class of materials did not receive sufficient attention until recently, when their potential was recognized in the emerging applications in photonics. Often the refractive index of the ferroelectric phase is high compared to silica, and therefore to minimize scattering losses, the size of FE crystallites must be in the nanometer range. To relax this requirement, recent attempts, principally in Japan, have shifted to systems based on tellurite (TeO_2) glass that has high refractive index ~2.24 [78-79]. The tellurite glass properties are briefly describe in subtopic 1. Mostly, the active component has remained one of the popular ferroelectric oxides viz. an alkaline-earth titanate of perovskite family like $BaTiO_3$ [80-81], an alkali niobate like $LiNbO_3$, a mixed alkaline-earth niobate of the tungsten bronze family like $Sr_{0.5}Ba_{0.5}Nb_2O_6$ (SBN), or an alkali tantalate like $LiTaO_3$.

In parallel, less common FE oxides have been considered for preparing TFGCs, if they can form glass without the need of adding another glass former. As the glass has the composition of a FE phase, it is hoped that devitrification can occur congruently with no change in local chemistry and hence the refractive index of the crystallites will be close to that of the matrix. Because of easy glass formability, the Stillwellite family of germinates like $LaBGeO_5$ is the leading composition in this class of TFGCs. By comparison, common FE oxides like $LiNbO_3$, $LiTaO_3$ and $PbTiO_3$, have been also prepared in amorphous state by rapid quenching, but then the material is in the film form.

ลิขสิทธิ์มหาวิทยาลัยเชียงใหม่
Copyright© by Chiang Mai University
All rights reserved

Considerable effort has been devoted recently for developing ferroelectric glass-ceramics for thin film capacitor, piezoelectric, FE random access memory, etc. applications where optical transparency is not important. Here sol-gel route of sample preparation has been particularly attractive due to its suitability for making thin films. As with melt-quenching glasses, FE phase is produced by heat treatment.

1) Tellurite glass

It has been known that tellurite or tellurium dioxide (TeO_2) is the most stable oxide of tellurium (Te), which has T_m of 733ºC [3, Appendix B]. This may be due to its special transition position between metals and non-metals. The stability of tellurium oxides has attracted many researchers in both crystalline solid and tellurite glass forms. The piezoelectric and photoelastic properties of paratellurite, a colorless tetragonal form of TeO_2, allows the potential usefulness of these compounds in ultrasonic-light deflectors. Moreover, these TeO_2 crystal have the extremely slow-shear wave propagation velocity of these crystals along the [110] direction, their low acoustic losses, and their high refractive index (n), which are applicable for using in laser light modulators. The tellurite structure are shown in Fig. 2.13.

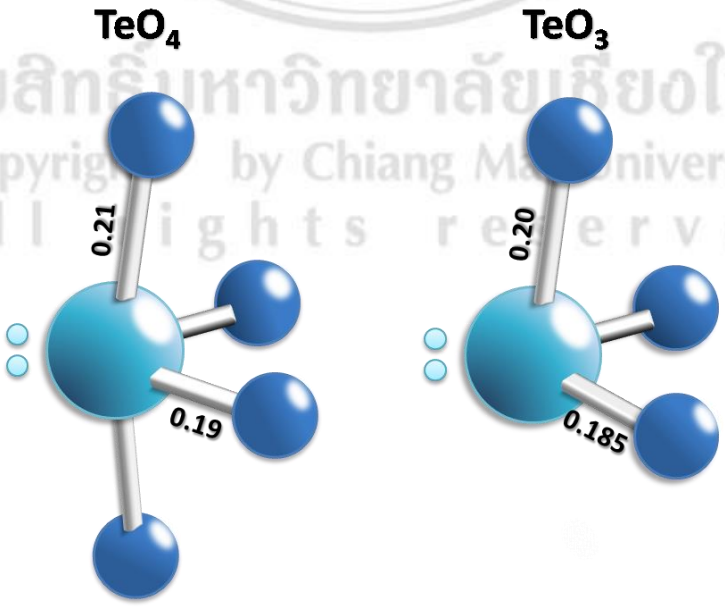

Figure 2.13 Tellurite glass structure [3].

ลิขสิทธิ์มหาวิทยาลัยเชียงใหม่
Copyright© by Chiang Mai University
All rights reserved

2) Silicate glass [82,67]

Silicate glass or silicon dioxide, also known as silica (from the Latin *silex*), is a chemical compound that is an oxide of silicon with the chemical formula SiO_2. It has been known since ancient times, that this oxide is the most commonly found in nature as quartz, as well as in various living organisms. Silica is one of the most complex and most abundant families of materials, existing in several minerals and being produced synthetically. Notable examples include fused quartz, crystal, fumed silica, silica gel, and aerogels. Applications range from structural materials to microelectronics to components used in the food industry.

In Fig. 2.14, the majority of silicates, the Si atom shows tetrahedral coordination, with 4 oxygen atoms surrounding a central Si atom. The most common example is seen in the quartz crystalline form of silica SiO_2. In each of the most thermodynamically stable crystalline forms of silica, on average, all oxygen atoms of the SiO_4 tetrahedra are shared with others, yielding the net chemical formula: SiO_2.

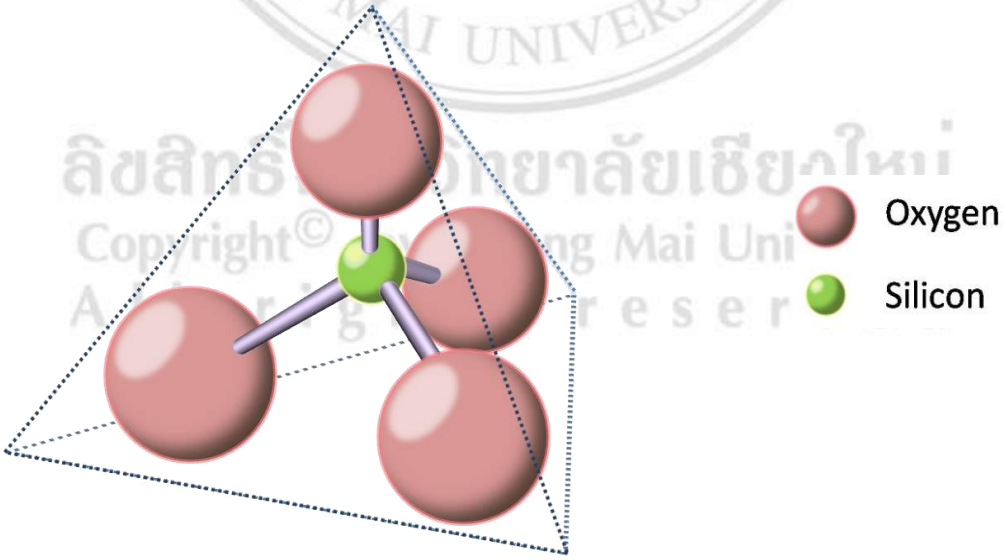

Figure 2.14 Silicate glass structure [67].

ลิขสิทธิ์มหาวิทยาลัยเชียงใหม่
Copyright© by Chiang Mai University
All rights reserved

2.3 Rare earth doped materials

Nowadays, the technology of telecommunication as displays, lasers, data storage and medical applications are particularly interested, due to the increasing demand for more comfortable and fulfilling lives [83]. This enormous demand lead to the requirement of new product innovation from new materials, in which will be the answer of the question "How can we improve those device efficiency?". The coincidence of luminescence rare-earth (RE) might be the answer of this question. The emerging of luminescence RE begin in the early of 20^{th} century. These interesting materials have a special characteristic. Their triple charge ions could activated the energy level in unused range to release the visible light or so called phosphors. The most well-known triple ions RE is erbium (Er^{3+}), europium (Eu^{3+}), terbium (Tb^{3+}) and cerium (Ce^{3+}), which can produce the intense visible light as red, green and blue colors [83,84].

In 1960s [83], RE doped glass and crystal become an attractive topic because of the development of solid state lasers, i.e. Nd-YAG system for laser applications, Nd-glass laser for high power applications and Holmium (Ho^{3+})-Praseodymium (Pr^{3+}) fiber laser for medical application. Until now, RE doped glasses and glass-ceramics are presented as the new era of opto-electronic application, which is used in wide applications such as telecommunication, optical memories and direct integration of display technology with semiconductor materials.

The intense study of Er_2O_3 as RE dopant began in 1980s. The most of research topics have been focused on this material because its emission band is around 1.53 μm, which is capable of applying with silica fibre for using in optical telecommunication. The important example application is erbium-doped fibre amplifer (EDFA). In addition, erbium not only useful for optical application but also applied in semiconductor systems (Si, GaAs, GaP and SiC) in order to create light emitting diode (LED). A.J. Kenyon [83] had summarized the behavior of Er^{3+} in various host materials as presented in Table 2.7. Moreover, applications of Er_2O_3 dopant are shown in Fig. 2.15.

ลิขสิทธิ์มหาวิทยาลัยเชียงใหม่
Copyright© by Chiang Mai University
All rights reserved

Table 2.7 Optical parameter of Er^{3+} in various solid host materials [83].

	Peak absorption cross-section (488 nm)	Peak absorption cross-section (980 nm)	$^4I_{13/2} \rightarrow {}^4I_{15/2}$ PL lifetime[a]	Upconversion coefficient	Peak-stimulated emission cross-section (1535 nm)	Luminescence bandwidth (1535 nm FWHM at 300 K)	Maximum optically active concentration
Silica [19]	$<8.0 \times 10^{-21}$ cm^2	1.0×10^{-21} cm^2	12×10^{-3} s	3.0×10^{-21} cm^2	7.27×10^{-21} cm^2	11 nm	0.1 at% (melt glass) (PECVD)
Phosphosilicate glass [19]		2.01×10^{-21} cm^2	10×10^{-3} s	9.0×10^{-21} cm^3 s^{-1}		27 nm	2.5 at%
Aluminosilicate glass [19,126]		3.12×10^{-21} cm^2	10×10^{-3} s	1.0×10^{-16} cm^3 s^{-1}	5.7×10^{-21} cm^2	43 nm	500 ppm
Silicon (crystalline) [19]	$2–8 \times 10^{-12}$ cm^2 (514 nm)		420×10^{-6} s				3×10^{17} cm^{-3}
Amorphous silicon [19]	1.4×10^{-14} cm^2 (514 nm)		800×10^{-6} s				
Silicon-rich silica [143]	7.3×10^{-17} cm^2	—	$\sim 2.5 \times 10^{-3}$ s (depends on Si content)			Up to 60 nm (depends on Si content)	—
Porous silicon [60]			1×10^{-3} s			~10 nm	
Alumina [19,191]		2.0×10^{-21} cm^{-2}	7.8×10^{-3} s	4.0×10^{-18} cm^3 s^{-1}	6.0×10^{-21} cm^2	55 nm	
GaN [120,114]		4.8×10^{-21} cm^{-2}	2.95×10^{-3} s			~8 nm	
GaAs			1×10^{-3} s		1×10^{-3} cm^2		7×10^{17} cm^{-3}
ZBLAN [172]					5.0×10^{-21} cm^2		18 mol%
Lithium niobate [19]			3.0×10^{-3} s	$<1.4 \times 10^{-19}$ cm^3 s^{-1}			
YAG				5.4×10^{-17} cm^3 s^{-1}			
PPMA [206]	1.1×10^{-20} cm^2		0.8×10^{-6} s			70 nm	
Tellurite [194,193,190,197]		4.48×10^{-21} cm^{-2}	3.3×10^{-3} s	2.74×10^{-17} cm^3 s^{-1}	1.3×10^{-20} cm^{-2}	80 nm	2.5 at%

[a] Maximum value reported in unclustered material.

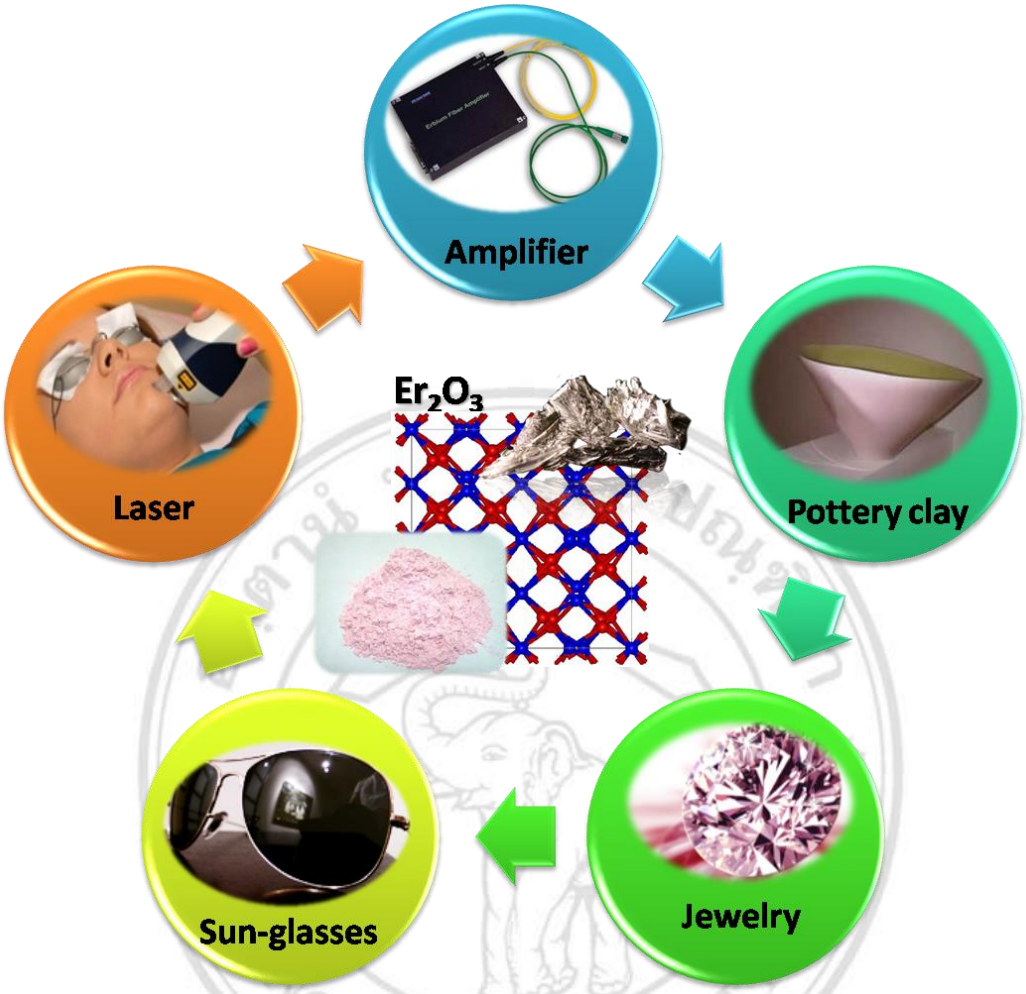

Figure 2.15 The Er_2O_3 dopants in various applications [143].

ลิขสิทธิ์มหาวิทยาลัยเชียงใหม่
Copyright© by Chiang Mai University
All rights reserved

The working function of RE doped materials can be described by their electronic structure. Fig. 2.16 represent the electronic structure of each trivalent RE element which is consisted of partially filled 4f shell and external fields of $5s^2$ and $5p^6$ subshell. Many studies found that the energy level of RE ions are insensitive to host environment, and after doped in crystalline or amorphous materials, the RE ions always show two or three plus charge ion. These ions are entering into the 4f shell rather than the external $5s^2$ and $5p^6$ subshell, and giving rise to the sharp emission spectra independent of the host materials. Thus, the transition of intra-4f electrons initiates the narrow band in the ultra-violet, visible, and near-infrared regions. There are some literatures talking about Er^{3+} dopant to ceramics, glass and glass-ceramics as following 3 sections (2.2.1-2.2.3).

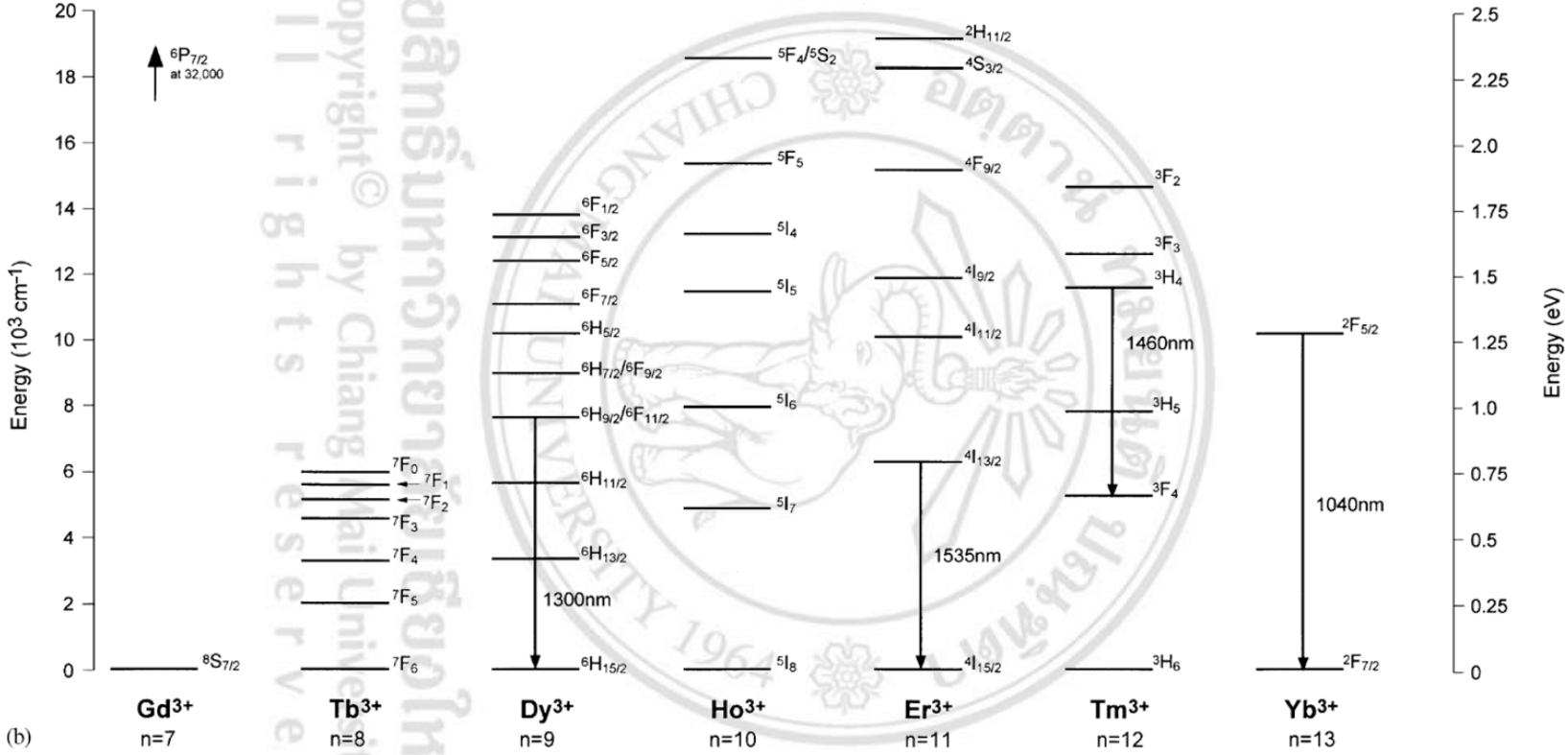

Figure 2.16 Energy levels of triple charge RE ions [83].

2.3.1 The effect of Er_2O_3 dopant on TeO_2 glass system

The effects of Er_2O_3 doped TeO_2 glasses on optical and mechanical properties have been reported in many papers. Here, we have reviewed correlated works done by various researchers.

In 2003, Hai lin et al. [85] studied the optical transition and up-conversion luminescence of Er^{3+} (1.0 wt%) doped Nb_2O_5-TeO_2 (NT) glass in order to develop optical fiber laser and amplifier. They found that the intense peak or IR fluorescence at 1.53 μm with full width at half maximum (FWHM) of 51 nm and visible up-conversion luminescence peak were observed under 975 nm and 798 nm (laser diode) excitation respectively. They also found that the up-conversion emitted light by using 2-photon absorption. In addition, the researchers also summarized the energy level of Er^{3+} ions in NT glass as shown in Fig. 2.17.

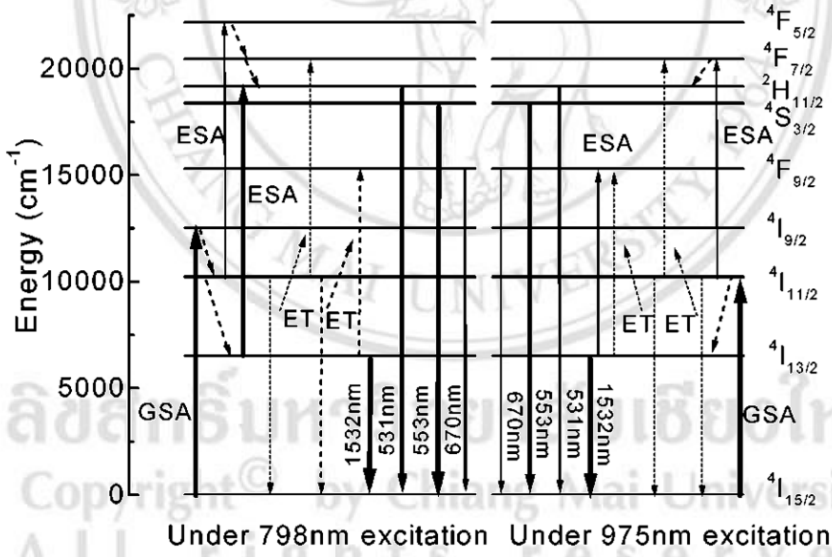

Figure 2.17 Energy level of Er^{3+} ions in Nb_2O_5-TeO_2 glass after applied 975 nm and 798 nm excitation source. GSA is ground state absorption, ESA is excited state absorption and ET is energy transfer [85].

Then, in 2005, Shixun Dai et al. [86] studied glass TeO_2-Nb_2O_5 system doped with 0.5 mol% Er_2O_3 ((100-x)TeO_2-xNb2O5, x=5-20) and summarized all data in Table 2.8.

ลิขสิทธิ์มหาวิทยาลัยเชียงใหม่
Copyright© by Chiang Mai University
All rights reserved

Table 2.8 Density, refractive index, concentration of Er^{3+} inside glass, glass transition - crystallization temperature and glass stability [86].

Glass composition	ρ (g/cm^3)	n_d ($\pm$0.02)	Er^{3+} concentration ($\times 10^{20}$ ion/cm^{-3})	T_g (°C)	T_x (°C)	$T_x - T_g$ (°C)
$95TeO_2$–$5Nb_2O_5$	5.290	2.04	2.01	374	466	92
$90TeO_2$–$10Nb_2O_5$	5.335	2.06	1.89	380	486	114
$85TeO_2$–$15Nb_2O_5$	5.416	2.07	1.81	405	544	139
$80TeO_2$–$20Nb_2O_5$	5.544	2.10	1.74	421	543	123
$70TeO_2$–$25ZnO$–$5Na_2O$	5.30	1.99	2.03	355	484	129

From their studies, the increase of Nb_2O_5 also increased density, refractive index and glass transition temperature in this glass system. It can be seen that the broad fluorescence spectrum was also found in telluride-niobic glass with higher amount of Nb_2O_5. The structural studies by XRD and Raman spectroscopy of glasses having more than 10 mol% Nb_2O_5 revealed that the substitution of Nb^{5+} in niobium octahedral site [NbO_6], leads to the increase in the strength of the glass in this system. In addition, the fluorescence life time of the $^4I_{13/2}$ was decreased while the emission cross-section for Er^{3+} : $^4I_{13/2} \rightarrow {}^4I_{15/2}$ was found to increase.

In 2009, R. Debnath et al. [87] attempted to synthesize the nanocrystals of $Er_2Te_4O_{11}$ in lead free fluoro-barium tellurite glass and study its up-conversion luminescence process. Their works indicated that aging time (or dwell time) is a significant factor in controlling the crystal size. They also confirmed that TeO_2 glass system was activated by Er^{3+} as resulted in absorption spectra of Er^{3+} band of around $^4I_{15/2} \rightarrow {}^2G_{9/2}$ and $^4I_{15/2} \rightarrow {}^4G_{11/2}$. The luminescence efficiency was increased of about three times after the growth of $Er_2Te_4O_{11}$ nanocrystals. This results show the prospect of its use as solar cell IR concentrator and NIR sensor.

Recently, in 2013, Goncalo Monteiro et al. [88] had studied the structural of Er^{3+} in $xGeO_2$-$(80-x)TeO_2$-$10Nb_2O_5$-$10K_2O$ glasses and glass-ceramics by using differential scanning calorimeter (DSC) to optimize the heat treatment temperature. The DSC results are shown in Fig. 2.18. XRD data in Fig. 2.19 revealed that this glass system has show several crystalline phases such as α-TeO_2, δ- TeO_2, GeO_2 (α-quartz), together with $K(Nb_{1/3}Te_{2/3})_2O_{4.8}$. In addition,

ลิขสิทธิ์มหาวิทยาลัยเชียงใหม่
Copyright© by Chiang Mai University
All rights reserved

their work also reported the structural data from Raman spectroscopy and Fourier transform infrared (FTIR).

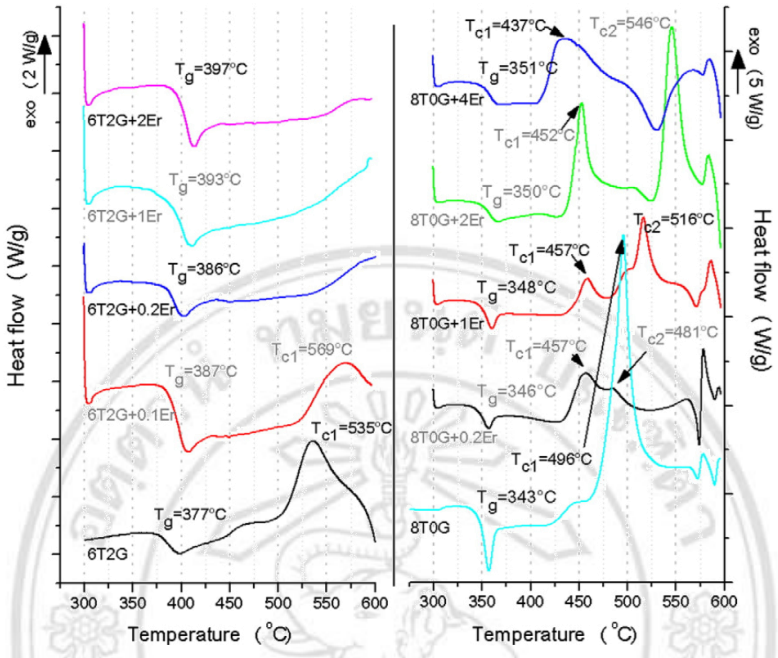

Figure 2.18 Thermal profile of $60TeO_2$-$20GeO_2$-$10Nb_2O_5$-$10K_2O$ (6T2G) and $80TeO_2$-$10Nb_2O_5$-$10K_2O$ (8T0G) with different mol% of Er_2O_3. (T_g=glass transition temperature, T_{c1} and T_{c2}=crystallization temperature) [88]

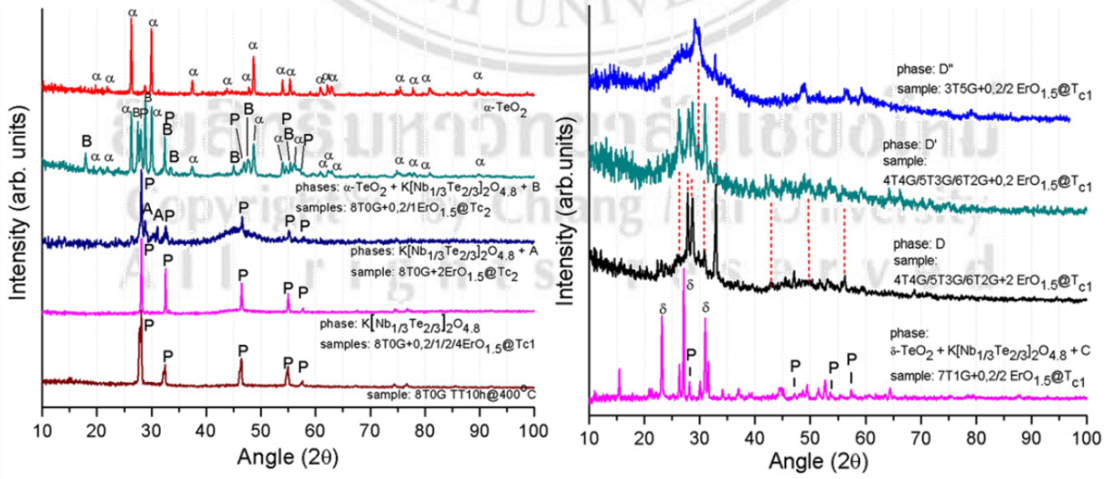

a. **b.**

Figure 2.19 XRD patterns of heat treatment sample. **(a.)** glass 8T0G systems with different percent of Er_2O_3, **(b.)** glass TeO_2 systems with different composition ranging from 30 – 70 mol% TeO_2 [88].

2.3.2 The effect of Er_2O_3 dopant on ceramics system.

In 2004, Sheng-Yuan Chu et al. [89] reported the effect of poling process to photoluminescence of Er^{3+} doped $KNbO_3$ ceramics. In this work, the electric field in poling process, poling time and annealing process were controlled in order to study the relation of photoluminescence phenomenon with those mention factors. The XRD results confirmed that no erbium cluster found in this work, which mean, the poling process did not change the structure of ceramics. After poling the ceramic samples show electron transition of $^4S_{3/2} \rightarrow {}^4I_{13/2}$. Moreover, this work also showed that the polarization and anneal process could modified the intensity of photoluminescence. In the other work, Cheng-Hung Wen et al. [90-93] had reported and discussed on the influent of Er^{3+} doped $KNbO_3$ ceramics. They found that erbium dopant has affected on sintering process [90]. The Er^{3+} dopants acted like sintering aid in which it is useful for $KNbO_3$ to form uniformity. However, the higher amount of Er^{3+} dopant (>2mol% Er_2O_3) could decrease the homogeneous of $KNbO_3$ form and create new phase transition [93]. After increasing sintering temperature, the Er^{3+} cluster that always occur in other ceramics was reduced. From SEM micrographs in Fig. 2.20 indicated that Er^{3+} dopant could inhibit the grain growth of $KNbO_3$ during sintering process. The optimize Er^{3+} doped $KNbO_3$ ceramics that activated the maximum intensity of photoluminescence is 1% of Er_2O_3. To improve the photoluminescence effect of $KNbO_3$ ceramics, the annealing treatment process was performed. From their report [91], the intensity of luminescence was increased with increasing annealing temperature as shown in Fig. 2.21. This results occurrence as annealing process could reduce the imperfection in $KNbO_3$ structure, and annealing process decrease hydroxyl groups in samples.

ลิขสิทธิ์มหาวิทยาลัยเชียงใหม่
Copyright© by Chiang Mai University
All rights reserved

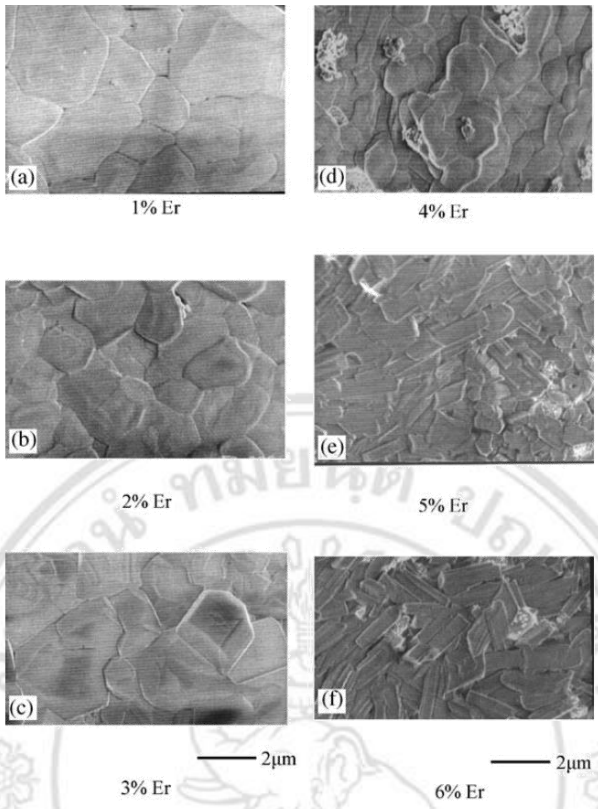

Figure 2.20 SEM micrograph $KNbO_3$ ceramic with different Er^{3+} percent dopants [90].

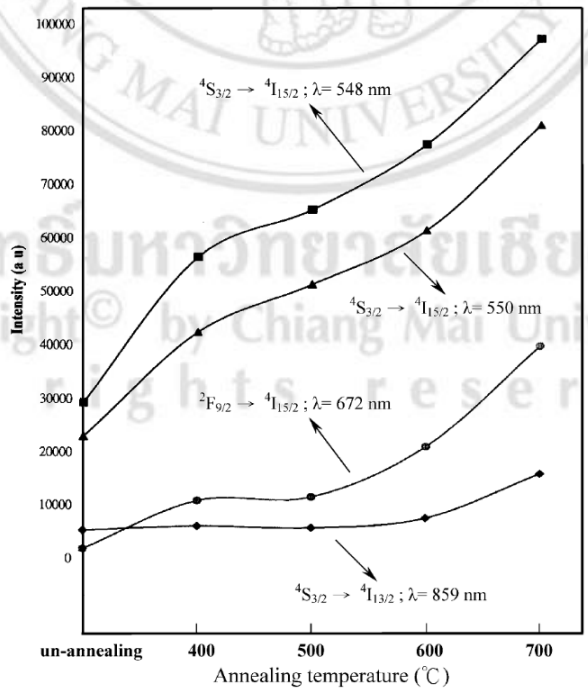

Figure 2.21 The effect of annealing temperature on photoluminescence intensity [91].

ลิขสิทธิ์มหาวิทยาลัยเชียงใหม่
Copyright© by Chiang Mai University
All rights reserved

Then, in 2014, the up-conversion luminescence of $K_{0.5}Na_{0.5}NbO_3$ ceramics doped with Er_2O_3 via solid state sintering has been investigated by H. Sun et al. [94]. The composition ratio of Er_2O_3 was varied between 0 – 0.05 mol%. From XRD analysis, the lower concentration than 1mol% of Er_2O_3 dopant ceramics showed KNN single phase, after increasing Er_2O_3 concentration than 1 mol%, the second phase occurred. This indicated that the optimize Er_2O_3 contents should be less than 1 mol% Er_2O_3 due to the limit of diffusibility of this RE type. Thus, the excesses of Er^{3+} (at higher content of Er^{3+}) which would not directly diffuse in KNN structure could resulte in impurity phase as shown in Fig. 2.22.

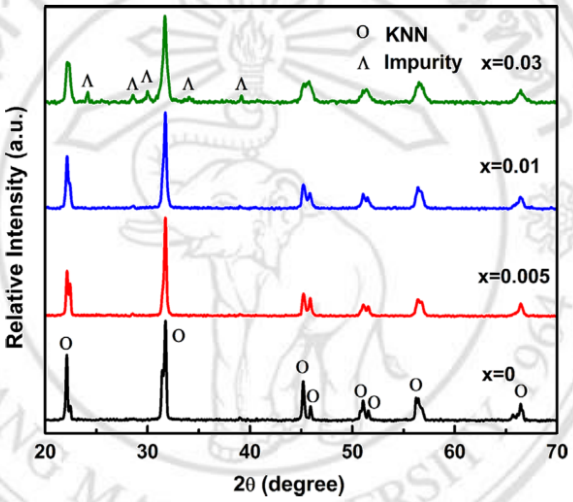

Figure 2.22 The XRD results of KNN doped with various Er_2O_3 contents [94].

The photoluminescence behavior of these ceramic systems after applying 980nm laser diode excitation source are shown in Fig. 2.23. It can be seen that the suitable Er_2O_3 concentration being able to activate the maximum intensity of up-conversion luminescence is 0.005 mol% Er_2O_3. From this figure, the luminescence consists of 2 emission band at around 510-590 nm (green light emission) and 645-695 nm (red light emission). Each emission band is associated with electron transition of 4f-4f level. In the first emission band (510-595 nm) is attributed to $(^2H_{11/2}, {}^4S_{3/2})\rightarrow{}^4I_{15/2}$ of Er^{3+} ions, while the second band (645-695 nm)is attributed to $^4F_{9/2}\rightarrow{}^4I_{15/2}$, respectively. The mechanism of electronic transition in KNN ceramic doped Er_2O_3 is shown in Fig. 2.24.

ลิขสิทธิ์มหาวิทยาลัยเชียงใหม่
Copyright© by Chiang Mai University
All rights reserved

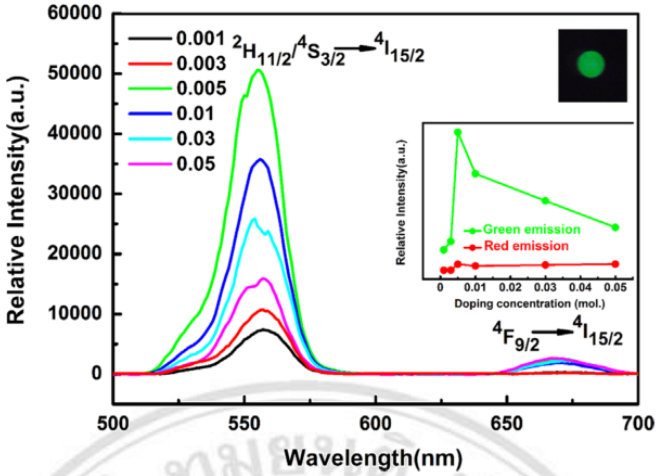

Figure 2.23 The up-conversion luminescence spectra of KNN ceramics doped with various Er_2O_3 content [94].

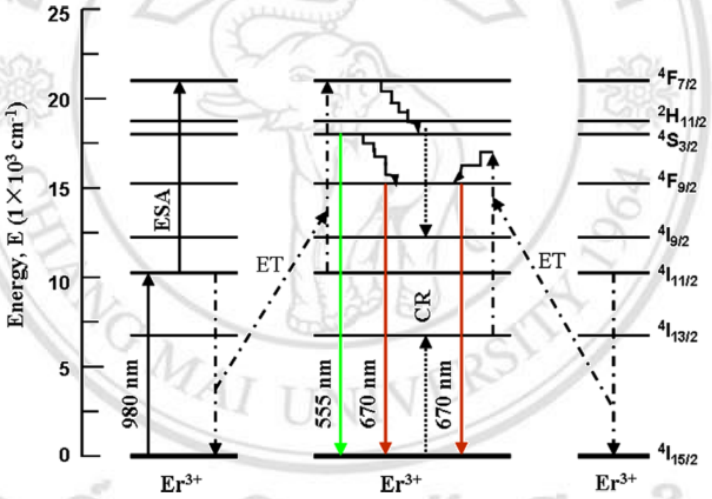

Figure 2.24 Energy level of KNN ceramics doped with Er_2O_3 [94].

ลิขสิทธิ์มหาวิทยาลัยเชียงใหม่
Copyright© by Chiang Mai University
All rights reserved

2.3.3 The effect of Er_2O_3 dopant on silicate glass system.

In 2010, R. S. Chaliha et al. [95] had reported the effect of Er_2O_3 dopant on optical and dielectric properties of K_2O–Nb_2O_5–SiO_2 glasses by heated at 800˚C for 0 – 100 h to obtain nanocrystals $KNbO_3$ in SiO_2 glass matrix. From XRD, SEM and TEM observations in Fig. 2.25, it was found that the average crystalline size of $KNbO_3$ crystals were in range 7-23 nm.

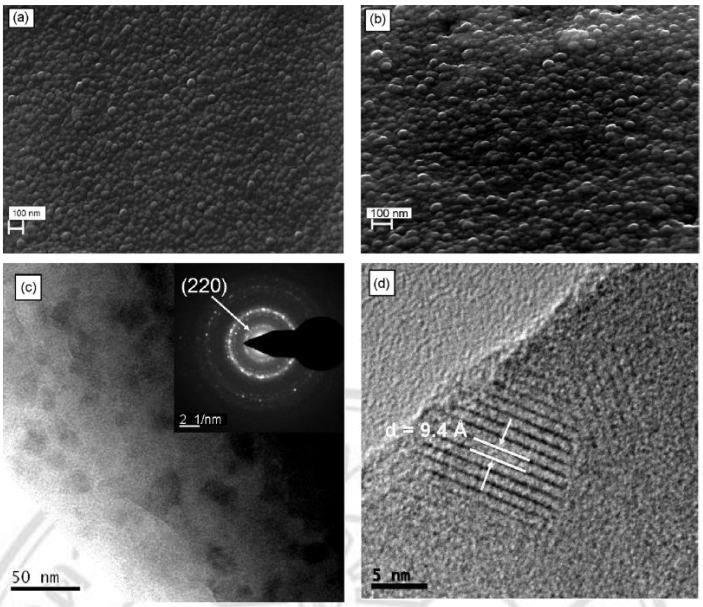

Figure 2.25 FESEM and TEM image of heat-treated glasses at 800˚C. **(a)** and **(b)** FESEM observed of glass heat treated for 3 h and 50 h, **(c)** and **(d)** SAED from TEM of glass heat treated for 50 h and HRTEM image of lattice fringe [95].

The dielectric property measurement was found to increase with increasing heat treatment temperature (Fig. 2.26). The dielectric constant increase sharply (from ε =17 to ε = 31) in heat treated samples. It is indicated that heat treatment process could generate the crystallization of $KNbO_3$ in silica rich phase and the further prolong heat treatments could increase the crystal size with higher dielectric constant (at 100 h, ε = 137) and spontaneous polarization (Ps = 0.41 C/m^2).

ลิขสิทธิ์มหาวิทยาลัยเชียงใหม่
Copyright© by Chiang Mai University
All rights reserved

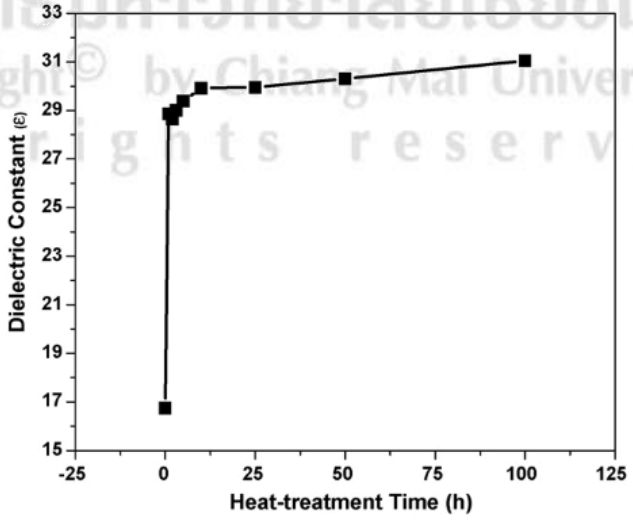

Figure 2.26 Dielectric constant of as-received glass and heat treated glass [95].

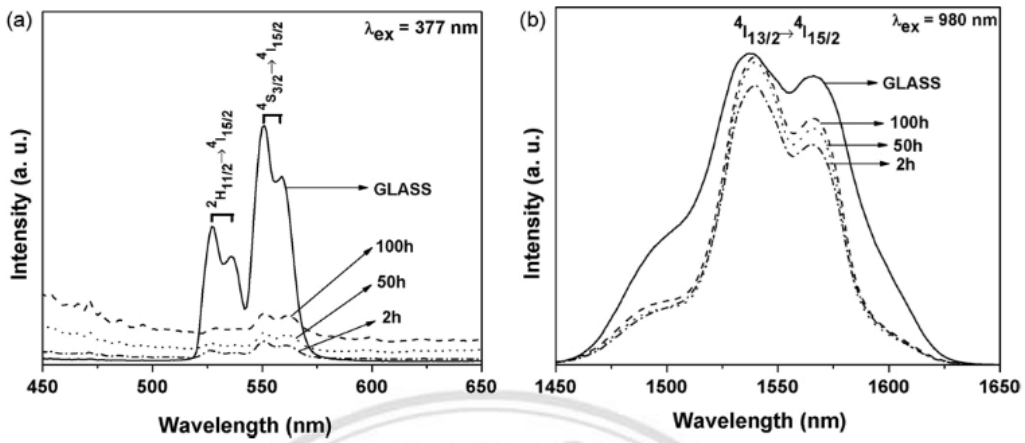

Figure 2.27 Photoluminescence measurement with different excitation source **(a)** λ_{ex}= 377 nm and **(b)** λ_{ex}= 980 nm [95].

In Fig. 2.27 (a), the obtained spectrum of the as-received glass which excited by 377 nm ($^4I_{15/2}\rightarrow{}^4G_{11/2}$) showed the intense visible light emission around 500 nm. This green emission around 515–542 nm and 542–577 nm corresponded to the $^2H_{11/2}\rightarrow{}^4I_{15/2}$ and $^4S_{3/2}\rightarrow{}^4I_{15/2}$ transitions respectively. While in Fig. 2.27 (b), as-received and heat treated glasses show emission band around 1550 nm on excitation at 980 nm ($^4I_{15/2}\rightarrow{}^4I_{11/2}$) which is an absorption bands of Er^{3+}ions. However, the study showed that the photoluminescence intensity gradually decreased with heat treatment time.

From many literature reviews, it can be clearly seen that there are scarcely reports on the effect of Er_2O_3 on KNN glass-ceramics. Thus, we have expected that this work may be helpful for anyone who interesting in the effect of RE on this glass-ceramics system.

ลิขสิทธิ์มหาวิทยาลัยเชียงใหม่
Copyright© by Chiang Mai University
All rights reserved